AD-A049 186 NAVAL RESEARCH LAB WASHINGTON D C F/G 4/1
ATMOSPHERIC TRANSMISSION MEASUREMENT PROGRAM AND FIELD TEST PLA--ETC(U)
NOV 77 J A DOWLING, R F HORTON, G L TRUSTY

UNCLASSIFIED NRL-8059 SBIE-AD-E000 081 NL

| OF |
AD
A049186

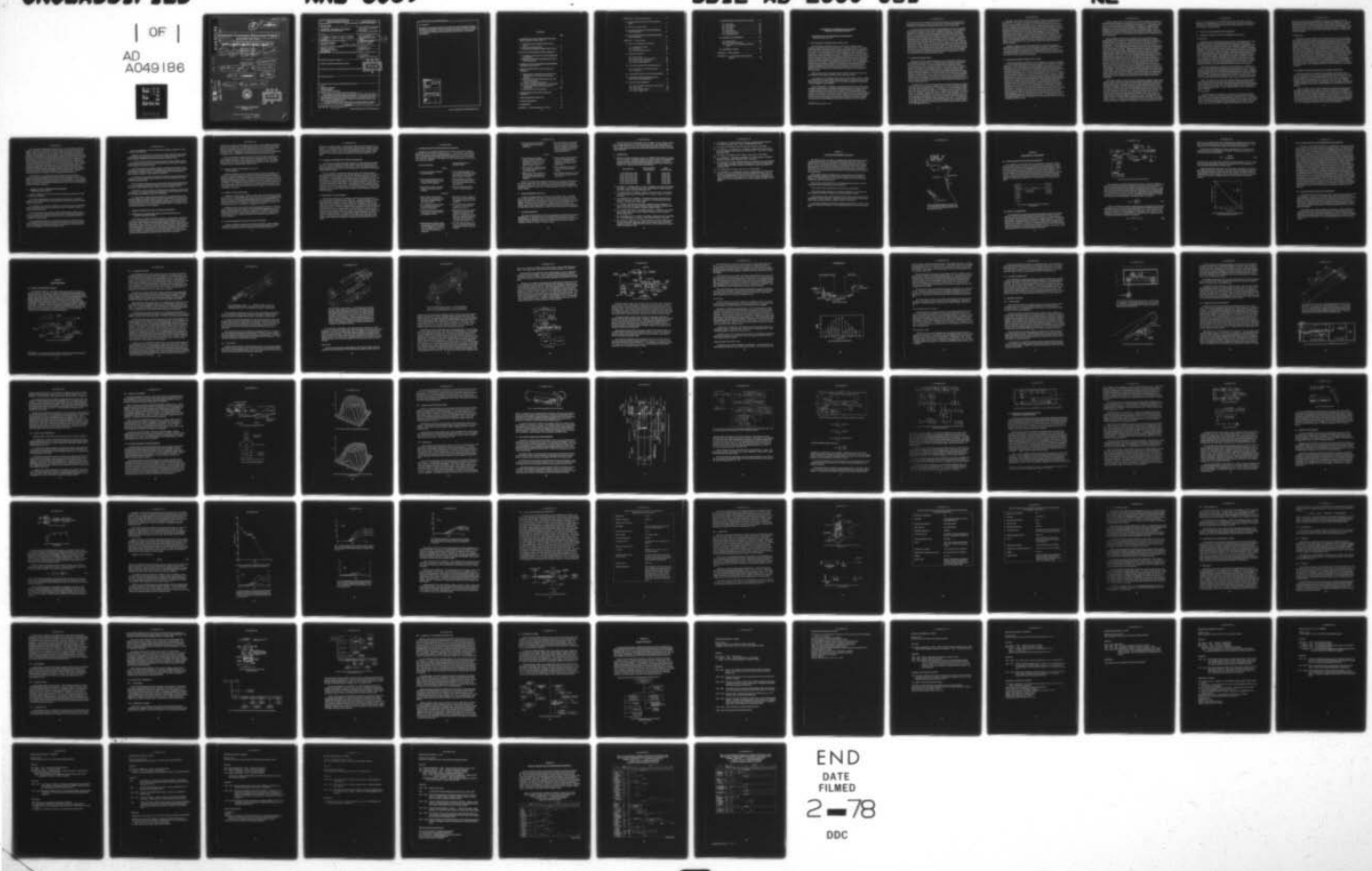

END
DATE
FILMED
2-78
DDC

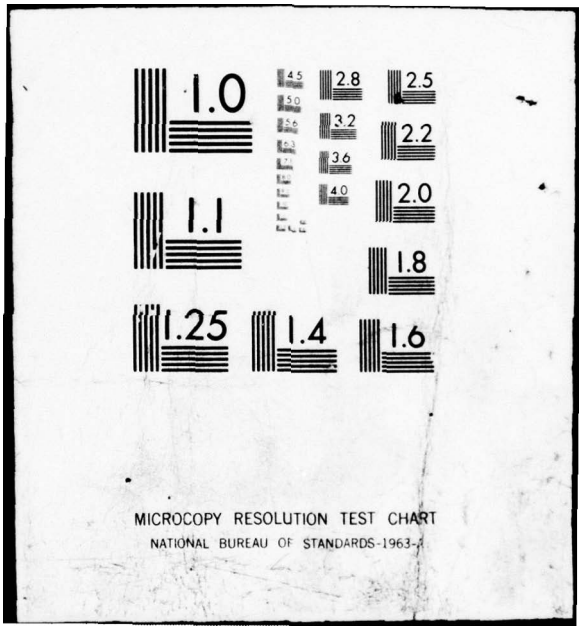
1.0
1.1
1.25
1.4
1.6
1.8
2.0
2.2
2.5
2.8
3.2
3.6
4.0
4.5
5.0
5.6
MICROCOPY RESOLUTION TEST CHART
NATIONAL BUREAU OF STANDARDS-1963-A

E000 081

12 p.

14 NRL [redacted]-8059

6

Atmospheric Transmission Measurement Program and Field Test Plan.

10

A. A. DOWLING, J. E. HORTON, G. L. TRUSTY, T. H. COSDEN, K. M. HAUGHT, J. A. CURCIO, C. O. GOTT, S. T. HANLEY, AND P. B. ULRICH

Optical Radiation Branch
Optical Sciences Division

James Richard Gary and Thomas Kenneth

W. L. AGAMBAR

Potomac Research Inc.
McLean, Virginia

16 S0182AA

9 Interim rept.,

17 S0182AA

11 30 Nov[redacted]977

12 90p.

18 SBIE

19 AD-E000 081

NAVAL RESEARCH LABORATORY
Washington, D.C.

251 950

SECURITY CLASSIFICATION OF THIS PAGE *(When Data Entered)*

REPORT DOCUMENTATION PAGE

READ INSTRUCTIONS BEFORE COMPLETING FORM

1. REPORT NUMBER: NRL Report 8059
2. GOVT ACCESSION NO.:
3. RECIPIENT'S CATALOG NUMBER:

4. TITLE *(and Subtitle)*: ATMOSPHERIC TRANSMISSION MEASUREMENT PROGRAM AND FIELD TEST PLAN

5. TYPE OF REPORT & PERIOD COVERED: Interim report on a continuing NRL problem

6. PERFORMING ORG. REPORT NUMBER:

7. AUTHOR(s): J. A. Dowling, R. F. Horton, G. L. Trusty, T. H. Cosden, K. M. Haught, J. A. Curcio, C. O. Gott, S. T. Hanley, and P. B. Ulrich

8. CONTRACT OR GRANT NUMBER(s): NRL Problem R05-31 63754N; Project 405-003-173-1-SRSL-40AA76

9. PERFORMING ORGANIZATION NAME AND ADDRESS: Naval Research Laboratory, Washington, D.C. 20375 — 17 SQ182AA

10. PROGRAM ELEMENT, PROJECT, TASK AREA & WORK UNIT NUMBERS: 16 SQ182AA

11. CONTROLLING OFFICE NAME AND ADDRESS: Department of the Navy, Naval Sea Systems Command (PM-22/PMS-405)

12. REPORT DATE: November 30, 1977

13. NUMBER OF PAGES: 89

14. MONITORING AGENCY NAME & ADDRESS *(if different from Controlling Office)*:

15. SECURITY CLASS. *(of this report)*: UNCLASSIFIED

15a. DECLASSIFICATION/DOWNGRADING SCHEDULE:

16. DISTRIBUTION STATEMENT *(of this Report)*

Approved for public release; distribution unlimited

17. DISTRIBUTION STATEMENT *(of the abstract entered in Block 20, if different from Report)*

18. SUPPLEMENTARY NOTES

19. KEY WORDS *(Continue on reverse side if necessary and identify by block number)*

Lasers
Atmospheric transmission
Fourier spectroscopy
Gas filter correlation spectroscopy

20. ABSTRACT *(Continue on reverse side if necessary and identify by block number)*

An atmospheric measurement program combining laser-line-extinction, Fourier-spectroscopy, and gas-filter-correlation-spectrometer experiments is described. A brief summary of the NRL experimental propagation effort since 1970 is presented followed by an abbreviated discussion of the current status of linear propagation modeling. Objectives of the current NRL atmospheric transmission measurement program are stated.

An experimental field test plan is presented followed by detailed information contained in several appendixes concerning procedures and facilities for laser-line-extinction measurements

(Continued)

DD FORM 1 JAN 73 1473 EDITION OF 1 NOV 65 IS OBSOLETE S/N 0102-014-6601

SECURITY CLASSIFICATION OF THIS PAGE *(When Data Entered)*

20. (Continued)

and calibrations, scanning-Michelson-interferometer experiments, gas-filter-correlation-spectrometer measurements, meteorological and aerosol data acquisition, and on-site data processing. Information concerning project staffing and a schedule for preparation and performance of a field experiment to be carried out at the Patuxent Naval Air Station, Patuxent River, Md., are contained in two final appendixes.

CONTENTS

ATMOSPHERIC TRANSMISSION MEASUREMENT PROGRAM AND FIELD TEST PLAN

1. BACKGROUND OF THE ATMOSPHERIC MEASUREMENT PROGRAM (1970 TO 1975)

1.1 NRL Experimental Propagation Effort (1970 to 1972)

The Naval Research Laboratory has been at the focus of atmospheric laser-propagation research during the past several years. A significant portion of the current body of knowledge of atmospheric effects on laser-beam propagation has been generated by work carried out at NRL during the years 1970 through 1975. This is especially true with respect to theoretical predictions of nonlinear atmospheric effects and experimental measurement of linear propagation phenomena. A reliable predictive capability for estimating nonlinear atmospheric effects on propagation mandates the use of accurate individual models for thermal blooming, turbulence, molecular and aerosol absorption, and aerosol scattering, including a description of significant interaction terms. The early strategy invoked by NRL in the pursuit of developing such models took the form of comprehensive thermal-blooming calculations carried out by numerical computation paralleled by an experimental program designed initially to answer questions concerning the turbulence spreading of large-aperture, focused laser beams and which has more recently been addressed toward a verification of molecular absorption predictions, particularly at DF laser wavelengths.

High-power-laser-device technology has driven the NRL program, which has consistently addressed issues rapidly surfacing as device technology unfolded.

A few examples of the interplay between NRL's activities and the evolution of high-power gas-dynamic and chemical laser devices demonstrate the contributions made to the Navy high-energy-laser (HEL) program by NRL, particularly regarding the understanding of HEL propagation in the atmosphere.

Paced by availability of a high-power CO_2 gas-dynamic laser source, the early NRL propagation program relied on a realistic theoretical modeling of the nonlinear interaction of a high-power beam with the atmosphere. Propagation experiments at high power awaited the installation and operation of a suitable CO_2 source. Meanwhile the theoretical program at NRL provided one of the first complete characterizations of nonlinear propagation available to the community, so that much of the knowledge concerning thermal blooming was on hand before costly high-power experiments were carried out. Questions regarding turbulence-induced beam spreading and beam wander specifically concerned with large-

Manuscript submitted August 31, 1976.

aperture focused beams were addressed by NRL during this period. The development of a Navy high-power propagation range was planned at the Chesapeake Bay Division of NRL (NRL-CBD) but was paced by completion of the Navy Tri-Service Laser (NTSL).

At the same time turbulence problems were investigated by low-power experiments which provided information early-on and at a significant reduction in cost compared to generating this information in the course of a high-power experiment. Experiments carried out by the NRL experimental propagation team during 1970-1972 at Webster Field, St. Inigoes, Maryland, verified that turbulence spreading of focused beams, while significant at visible wavelengths was a secondary factor at 10.6 μm [1-3]. These same experiments showed that beam wander phenomena could be explained by geometrical optics and that the wander phenomena were sufficiently slow so that wander correction using adaptive optics is feasible. The NRL work by no means was the only experimental studies of these effects; however the focused-beam measurements performed by the NRL field-measurement team provided the first data available to the HEL community from an extensive series of tests using moderately large aperture optics and which were supported by extensive micrometeorological data. A data base was generated in these tests sufficient for a useful comparison to theoretical estimates of the range, wavelength, and C_n (turbulence) dependence of focused-beam spread and wander.

1.2 Experimental Planning (1973)

While data were being analyzed subsequent to the focused-beam experiments, detailed planning was under way for an overwater high-power propagation range adjacent to the NTSL at NRL-CBD. These plans included extensive micrometeorological monitoring stations on shore as well as a multilevel, tower-mounted station on the jack-up-barge (JUB) high-power target diagnostic station. During this period (principally CY 1973) a major redesign of the equipment used in the low-power propagation tests described earlier was undertaken. The focused-beam-spreading data showed that nearly diffraction limited propagation was observed at 10.6 μm in the earlier tests for moderate turbulence at ranges up to 1.75 km. With the objective in mind of reducing diffraction spreading at CO_2 wavelengths and carrying out the measurements at longer ranges and at additional infrared wavelengths, a new low-power optical transmitter design was produced, with an increase in telescope aperture from 40 to 91 cm along with the inclusion of a CO laser operating near 5 μm.

The rapid advance in device technology which came about during this time caused a major impact upon the planning and implementation of the NRL propagation programs in both the high- and low-power areas. The preparation work for the high-power propagation range was thoroughly reevaluated. It was decided to redirect this effort toward the use of a high-power DF laser rather than to complete range preparations at CBD and carry out a propagation program there using the NTSL at CO_2 wavelengths. The choice of DF as the principal wavelength of interest for the Navy HEL program based on predicted propagation advantages over CO_2 was made about this time, and the redirection of the NRL high-power propagation effort responded to this choice. Accordingly plans for the range and experiments at the NTSL were terminated and the emphasis shifted toward planning a high-power experiment using the Baseline Demonstration Laser (BDL) at the TRW Capistrano test site.

The impact of the switch to DF was also felt in the low-power propagation program about this time. One of the most important propagation questions at the time with regard to the Navy program was whether or not the theoretical predictions of very low molecular absorption at DF wavelengths were true. Realizing that the system planned for use in the extended turbulence beam-spread studies could be readily modified for measurements of atmospheric transmission and thus provide answers to that question, the NRL field-measurement team set about this task. With the help of the Air Force Weapons Laboratory, a small CW DF laser was obtained and designed into the new NRL large-aperture-telescope transmitter. Operation of this laser required an additional trailer housing a 42-m^3/min (1500-cfm) vacuum pump required to produce a supersonic flow in the laser gain region and necessitated the careful design and use of a fluorine-gas supply system. The conceptually simple DF laser uses a precombustor burning H_2 and F_2 to generate the excited fluorine atoms, and therefore requires these rather elaborate supporting equipments.

Planning for high-power tests at TRW was started, and much of the diagnostic instrumentation originally planned for the CBD range was modified to operate at 3.8 μm for use in the TRW tests. In the meantime the primary emphasis in the NRL in-house experimental propagation program became one of fielding the DF-laser transmission experiment with the objective of providing a real-world check of the propagation predictions upon which the Navy's HEL strategy was being planned.

1.3 Experimental Propagation Program (1974 to 1975)

The first long-path field measurements of DF propagation by any group were carried out by the NRL field-measurement team at Cape Canaveral Air Force Station in February-March 1974. Several measurements of absolute transmission were made on two of the strongest lines in the output spectrum of current high-power DF chemical lasers along with measurements on two other DF lines. Preliminary observations of near-simultaneous focused-beam spreading at 0.63, 3.8, and 10.6 μm were made along with a series of transmission measurements for 17 CO_2 laser lines between 9.2 and 11.0 μm. A comparison of transmission measurements on the $P_2 7$ and $P_2 8$ DF lines for a variation in absolute humidity between 10 and 16 torr of water vapor showed no marked discrepancies with predicted values, demonstrating that the high transmissions predicted at these wavelengths could in fact be realized in the real atmosphere [4]. The beam-spread data obtained at that time was consistent with predictions based on the earlier tests and theoretical estimates; however, only rather-low-turbulence conditions persisted during these measurements [5, 6]. The results of the CO_2 measurements were compared to calculations performed for NRL by R. K. Long, Ohio State University, for the conditions of the measurement. The results of this comparison indicated that the model used for the water-vapor continuum absorption in the 9-to-11-μm region could be inaccurate. Follow-on measurements were planned for May-July 1974 to collect more data for each of the above investigations, once the transmitter telescope optics had been recoated, having suffered appreciable degradation in the salt-air environment. An unfortunate series of circumstances delayed the optical refurbishment for several months, causing a cancellation of the planned follow-on tests.

The data available after the 1974 measurements provided a preliminary validation of predicted molecular absorption coefficients for the $P_2 7$ and $P_2 8$ DF lines and spot checks on two other lines but did not provide sufficient information for a comprehensive comparison to theoretical predictions of transmission for a high-power multiline DF laser operating over a wide range of absolute humidities. Accordingly a repeat of the DF transmission experiment was planned once the optical system was repaired. During the rebuilding period several major improvements in the extinction measurement system were designed and incorporated, so that this several-month period was not an inefficient loss of time or momentum.

The DF transmission experiment was repeated at Cape Canaveral AFS during February-March 1975. By this time an improved DF laser operating with an intercavity grating had replaced the earlier one. An important feature of this new laser was provision for rapid selection of any 22 DF lines with an output of 0.5 watt TEM_{00} on the strongest lines. Another significant improvement in the experiment was realized by the incorporation of a GaAs optical data link for relaying the laser reference power along the 5-km overwater path in real time. Using these improvements, transmission measurements on any of the 22 DF lines could be obtained within several seconds of one another. During this second Florida experiment emphasis was placed on collecting a data base sufficiently large so that an effective test of theoretical transmission predictions for the 22 lines studied could be made. As a result, turbulence-effect measurements at 3.8 μm and transmission measurements at 10.6 μm were deferred until future experiments. During an 8-week operating schedule nearly 400 individual transmission measurements on 22 DF lines plus Nd-YAG at 1.06 μm were obtained for a water-vapor pressure variation between 4 and 20 torr (0.5 and 2.7 kPa). Subsequent comparisons to theory have pointed up certain inaccuracies in the Air Force Cambridge Research Laboratory line atlas used as the basis for predictions of laser line transmission. These inaccuracies are being rectified by an interaction between NRL and Science Applications Inc. (SAI), Ann Arbor, Michigan. The latter group is presently performing high-resolution measurements of HDO, N_2O, and CH_4 molecular absorption in the DF laser region on contract to NRL so that revised parameters may be included in the AFCRL data tape where appropriate. Several revisions in line strengths for certain HDO lines have already been generated by this program and have produced improved agreement between theory and the NRL Florida data.

With primary emphasis in the NRL in-house experimental propagation program being directed toward DF extinction studies, the high-power DF measurement experiment was fielded jointly by NRL and teams from the Army Ballistic Research Laboratory (BRL) and Lincoln Laboratory. The NRL involvement was principally specification and procurement of the high-power measurement instrumentation, and the actual measurements were carried out by the Army team. The NRL field-measurement team carried out low-power DF transmission measurements in conjunction with the high-power DF tests conducted during the Joint Army Navy (JAN) propagation program. The low-power extinction measurements were performed in-situ at TRW, so that representative experimental values for molecular absorption occurring at the time of the high-power tests could be obtained. In addition these measurements provided an extension of the earlier Florida data base to an environment influenced by the local western coastal aerosol distributions, an important consideration in interpretation of the JAN experiment and in the

extension of the modeling of DF transmission based on the Florida data. Using the equipment and techniques proven out in the earlier Florida tests, nearly 600 transmission measurements on the 22 DF lines plus 1.06 μm were taken during the 14-week period from mid-June through September.

2. STATUS OF LINEAR PROPAGATION MODELING

2.1 Atmospheric Transmission of the Three High-Energy Laser Systems

DF Wavelengths

Propagation at DF wavelengths has received intensive study during the past 3 years. McClatchey and Selby [7] first published predictions based on the AFCRL data tape which showed that molecular absorption at DF wavelengths was substantially lower than all predictions for CO_2 and most CO laser lines. Subsequent calculations by Long, Mills, and Trusty [8] included the water continuum omitted by AFCRL, but predicted transmission was still high. Spencer [9] reported laboratory measurements for individual atmospheric constituents for several DF lines and others have reported additional calculations. Laboratory measurements were hampered in that small molecular absorption in the DF region results in high ($> 95\%$) transmission for ambient atmospheres and paths of $\lesssim 1$ km, about the maximum obtainable in the laboratory. In addition to a real-world verification of extinction at DF frequencies with the inclusion of aerosol effects, part of the motivation behind the NRL measurements that were described in the background section was to carry out accurate measurements over a 5-km path, in order to better see the effects of such weak absorption barely detectable in the laboratory.

The NRL measurements have provided an extensive data base for comparison to modeling. Certain disagreements with predictions were identified as a result. Using the output of the SAI, Ann Arbor, high-resolution laboratory spectroscopy now in progress, the remaining discrepancies are now being systematically addressed. Molecular absorption at DF frequencies is currently much better understood than it is for either CO or CO_2 laser lines. The largest remaining uncertainty has to do with an accurate picture of the small water-vapor continuum in the DF region, particularly its temperature dependence.

Based on an analysis of the 1975 Cape Canaveral AFS data, the ability to predict aerosol scatter on these same DF laser lines, using only a meteorological observation (aerosol distribution) is in poor shape. Substantial instrumental and procedural questions must be answered before aerosol extinction modeling approaches the success realized for molecular absorption predictions. A more detailed discussion of these observations is given in Appendix C.

CO_2 Wavelengths

Molecular absorption is conceptually much simpler in the 9-to-11-μm region and dominated by a water-vapor continuum at sea level. Early measurements by Rensch, McCoy, and Long [10] yielded a molecular-absorption value of 0.4 km^{-1} for midlatitude summer conditions, and laboratory data for H_2O absorption in this region seems to bear this out. The temperature dependence of the continuum is still a question, and recent analyses [11] based on data taken in England by EMI Electronics Ltd. have raised

questions concerning the current LOWTRAN-3 computer-code modeling for this continuum based on earlier measurements by Burch, Singleton, and Williams [12]. The NRL measurements between 9.2 and 11.0 μm during the 1974 Florida experiment showed a consistent variance with calculations supplied by Long using the continuum based on the measurements by Burch et al. A field-data base comparable to that now available for DF would resolve many of these questions and would provide information on aerosol effects at these wavelengths.

CO Wavelengths

Atmospheric molecular absorption for low vibrational levels in CO is more poorly known than for either of the other two HEL systems. Just as in the case of DF, AFCRL [13] produced the earliest predictions, followed by Ohio State University [14]. Long's subsequent measurements for some of the higher vibrational lines showed a marked disagreement with predictions. Unlike the CO_2 region, where the local line structure is relatively unimportant and the H_2O continuum dominates, and unlike the DF region, where there is a substantial mix of many relatively weak local lines plus weak N_2 and H_2O continua, the CO region is a case of picking one's way through the tulips. In the DF region local line absorption is important only for a few near-coincidences of DF lines with the core or center of a weak local line (N_2O, HDO, CH_4). In the CO region absorption varies drastically from line to line depending on whether or not the CO lines *miss* the cores of the strong local lines. When they do, transmission is favorable, but the absorber line shape away from the line core is important, and this is not well understood. Line shapes are more predictable near the line centers than far out ($\gtrsim 10$ halfwidths) from the line center. Thus confidence in molecular absorption predictions for CO laser lines is lower than that for comparable predictions in the DF region prior to experimental verification.

2.2 Broadband Transmission Measurements and Atmospheric Spectroscopy

The early predictions of atmospheric laser transmission referenced the work of Taylor and Yates [15] before it soon became apparent that there was little point in trying to use spectroscopy of the atmosphere performed with $\gtrsim 5\text{-cm}^{-1}$ resolution to infer what the transmission of a laser line 10^{-4} to 10^{-5} cm^{-1} wide would be propagating through an array of quasi-randomly located pickets about 0.1 cm^{-1} wide. Since this landmark atmospheric data proved to be inapplicable to laser transmission problems, high-resolution calculations were invoked, and their application to the problem has just been discussed.

There is currently a need to perform high-resolution transmission measurements in the infrared atmospheric windows and to correlate this information with appropriate supporting meteorological data including aerosol data. Presently the Army Night-Vision Laboratory and Air Force Geophysics Laboratory (formerly AFCRL) are collecting broadband IR transmission data (program OPAQUE). The broadband data are of limited use for some of the more sophisticated spectral discrimination concepts now being proposed for IR target identification and of even less use for reliable laser-transmission predictions. Yet, at the same time, the technology exists for collecting moderately high resolution (≈ 0.1 cm^{-1}) atmospheric absorption spectra useful for both applications.

The combination of high-resolution spectroscopy over long atmospheric paths performed in conjunction with absolute transmission measurements at the three laser wavelengths of current interest (DF, CO, and CO_2) simultaneously address a wide variety of interests within and beyond the HEL community. This complementary measurement program now being planned by the NRL field-measurement team will provide the needed input data for verification of molecular absorption models for CO and CO_2 as well as DF. The combination of continuous high-resolution spectra as opposed to a sampling at 22 discrete fixed frequencies will provide additional information for use in separating continuum molecular-absorption phenomena from aerosol scattering effects. Each is weakly wavelength dependent, and observations of the true minimum absorption values between local lines in combination with measurements of aerosol particle concentrations and absolute humidities will provide a means for handling this problem heretofore lacking. Evaluations of infrared tracking and imaging systems in certain instances require information at higher resolution than that available in the *LOWTRAN-3* model. The high-resolution spectra to be produced by the NRL program addresses this need.

A vital feature of the complementary laser-transmission and high-resolution-absorption measurement program which has not yet been emphasized is that the laser absolute transmission measurements will provide an absolute calibration for the continuous spectra. The uncertainties of geometrical corrections normally applied to long path transmission measurements using collimated blackbody sources with "known" beam divergences should be minimized accordingly.

3. SUMMARY OF THE ATMOSPHERIC MEASUREMENT PROGRAM (1970 TO 1975)

Major accomplishments of the NRL experimental propagation program from 1970 to 1973 were the following:

- The NRL field-measurement team performed the first extensive experiments designed to study turbulence-induced beam-spread and wander phenomenology for large-aperture focused beams;

- Consistently in the NRL field experiments, as is required in any field experiment, sufficient supporting meteorology was monitored in order to successfully compare the results to theoretical models;

- The measurements taken during the Webster Field, Maryland, studies were sufficiently extensive and the subsequent analysis performed was adequately thorough such that the minimal impact of turbulence spreading at 10.6 μm on high-energy-laser (HEL) propagation was demonstrated;

- An experimental model for the wavelength dependence of turbulence-induced beam spreading and beam wander was obtained in the NRL studies which was available for use in estimating the relatively more important contribution of these effects at 3.8 μm once DF propagation for the Navy became a reality.

Major accomplishments of the NRL experimental propagation program from 1973 to 1975 were the following:

- Building on the field experience with the use of adapted laboratory laser sources in combination with large-aperture, precisely pointable optical systems, the NRL field team successfully designed and fielded the present laser transmitter system;

- A state-of-the-art CW DF laser and associated fluorine supply and large vacuum pumping station were incorporated into the field equipment and successfully operated in a one-of-a-kind field measurement system;

- The NRL experimental propagation program was sufficiently responsive to Navy HEL-program developments such that the instrumentation intended for turbulence propagation studies was instead modified to perform DF extinction measurements and was used extensively thereafter in three major field experiments;

- Conformance with favorable transmission predictions for important DF laser wavelengths in the real atmosphere was first observed by the NRL field-measurement teams in February and March 1974;

- Recent extensive measurements by this same group has provided a large data base for use in accurately modeling DF transmission in-so-far as molecular absorption is concerned and in determining the range of variation in aerosol scattering at 3.8 μm;

- Maintenance of an interchange of information between laboratory and field efforts has resulted in a converging process whereby discrepancies in molecular-absorption modeling are systematically yielding to improved understanding;

- A high-resolution interferometer-spectrometer system (scanning Michelson interferometer, SMI) and a gas-filter correlation spectrometer (GFCS) have been specified and are being designed into the NRL field-measurement program. These instruments used in conjunction with fixed-frequency laser transmission measurements in the regions from 3 to 5 μm and from 9 to 11 μm will provide a substantial increase in our ability to understand infrared transmission in the atmosphere.

4. PRESENT OBJECTIVES OF THE PLANNED NRL PROGRAM

4.1 High-Resolution Atmospheric Spectroscopy Using Fixed-Frequency-Laser Absolute Transmission Calibration

The concept of an absolute transmission calibration of high-resolution atmospheric spectroscopy using fixed-frequency laser wavelengths was already alluded to in Section 2; it represents a major thrust in the experimental propagation program currently being implemented at NRL. Building on the experiences gained in the three major field experiments already described, the present tack represents an intensification of these studies rather than change of course or emphasis in the program. Fixed-frequency measurements at laser wavelengths as exemplified by the recent DF measurements in Florida are of obvious importance in the near term to the Navy HEL program. Molecular-absorption modeling at these wavelengths is apparently well in hand as a result of these

measurements combined with the results of other work. Aerosol modeling on the other hand is not well understood. The high-resolution spectra to be obtained in the field program now in preparation will provide an additional dimension for aerosol study by permitting quantitative measurements of trough extinction due only to aerosols and molecular continua. Quantitative high-resolution spectra will have important ramifications for validation of both LOWTRAN as well as high-resolution calculational models.

In essence the planned measurements will provide the data which heretofore have long been needed but have not been forthcoming. Using these data, one can achieve direct, effective verification of laser transmission and broadband models. The measurements will provide an effective means for assessing the influence of weak absorptions, discernible only over long atmospheric paths ($\gtrsim$ 5 km).

4.2 Extension of DF-Laser Measurements to CO_2- and Laser Wavelengths

Once the techniques for using the scanning Michelson interferometer (SMI) in concert with DF measurements have been practiced in the field and the required learning experiences obtained, a straightforward extension of these measurements to the CO_2 and CO laser operating regions is planned. Minor modifications to the SMI optical head (long-wavelength IR beamsplitter and detector package) are required for operation in the 9-to-11-μm region. A low-vibrational-transition CO laser source is required for operation in the 4.7-to-5.0-μm region. Plans are now being made to accelerate the procurement of such a laser from FY 1977 into FY 1976 (plus the transition quarter), so that it may be used in the field in the near term.

4.3 Gas-Filter Correlation Spectrometer

In addition to the SMI effort a gas-filter correlation spectrometer (GFCS) now being built by SAI, Ann Arbor, Michigan, will be used in the field. The original design goal for this device was as a method for obtaining path-integrated water-vapor measurements. By using a local reference cell filled with HDO rather than H_2O and relying on the known isotopic ratio of D/H in the atmosphere, an effective path-concentration product of ambient water vapor over a 5-km path can be obtained in a 1-m cell.

In addition to this concept, which was the original reasoning behind the GFCS, the device is interesting from the standpoint of being a single-ended diagnostic tool for propagation path characterization. Using the sun instead of the blackbody source in the optical transmitter trailer, a single-ended measurement can be made. Eventual development of this device into a shipboard package for HEL propagation-path definition is worth consideration.

4.4 In-House Atmospheric-Transmission Computer-Code Capability

To make comparisons of theoretical transmission calculations to values measured during field tests, an in-house high-resolution code calculational capability is required. Until now this need has been met by consultive services provided as a task in a

spectroscopic modeling contract. This procedure suffers in terms of response time and flexibility. It is highly desirable for rapid analysis of field data that a hands-on, in-house predictive code be available. This need is being addressed as a task in the SAI measurements/modeling contract currently under way and should thereby be satisfied. Such a capability will be critically needed once high-resolution spectra are generated in the field.

4.5 Complementary High-Resolution Laboratory Measurements

In the DF case, discrepancies between calculations and field measurements pointed up errors in HDO line strengths and widths entered on the AFGL data tape, and it is likely that a similar situation exists in the CO region. Hence a laboratory-measurement program addressing the verification of H_2O-line parameters will be needed to back up the field-measurement program.

The CO_2 transmission measurements during the NRL 1974 Florida experiment showed that extinction on the R_{30} line of the 001→020 band near 9.2 μm was 0.27 km^{-1} for conditions such that extinction on the P_{20} line of the 001→100 band at 10.6 μm was 0.44 km^{-1}. The advantages of operating CO_2 lasers at wavelengths near 9 μm in the atmosphere have not been fully explored. Earlier laboratory data [16] showed that CO_2 and H_2O line widths in this region are not accurately represented on the AFGL tape in all cases, particularly for high J values. A thorough study of CO_2 propagation using laboratory data to provide information for modeling improvements dictated by field measurements is in order in this spectral region also. This is particularly true considering that significant effort is currently being devoted to pulsed CO_2 laser development within the Navy HEL program.

4.6 Improvement of Aerosol Modeling

The fact that aerosol-extinction modeling is nowhere near as well understood as molecular-absorption modeling has been pointed out. A detailed description of the problems experienced in attempts to go from a measured aerosol-particle distribution to a prediction of optical extinction is given in Section C6 of Appendix C. This is a first-order problem; aerosol effects can dominate extinction on several important DF lines in a maritime environment. Currently a reliable predictive capability for aerosol extinction of an infrared beam is lacking. Improvements in instrumentation and experimental techniques directed toward this capability are needed. Large sampling volumes yielding good statistics for larger particles and an in-situ refractive-index measurement of ambient maritime aerosols are required. The planned NRL program will address both of these issues in a continuing manner, supporting the optical transmission measurements and using the added information resulting from the high-resolution spectral data to be obtained.

5. JUSTIFICATIONS FOR THE PLANNED NRL PROGRAM

Expressed as well as implied justifications for the NRL experimental propagation program have been set forth in the preceding sections. In this section a concise restatement of these points is made by a specific address to several of the key issues identified in the recent HEL Review Group PSP Third Plenary Session, held on 17-18 November 1976 at the Mitre Corporation. With regard to the PSP recommendations, the following items should be considered:

PSP Recommendation	Corresponding Element of the NRL Program
General	
• CO sources should be developed and made available	• A low-vibrational-transition CO source has been identified; procurement thereof has been advanced from FY 1977 to FY 1976
• FTS (Fourier transform spectroscopy) instruments should be made available for field programs	• This is integral to the portion of the NRL FY 1975-1976 special laser technology development program (SLTDP).
• Instruments to monitor the distributions of molecules should be developed	• GFCS to be delivered and evaluated in the planned program
Field Data	
• High-resolution FTS extinction data should be accumulated in the three major wavelength regions (CO, CO_2 and DF).	• This type of work is in NRL's program and is not being addressed in comparable depth by any other laboratory
• CO fixed-frequency data comparable to existing DF field data should be accumulated	• CO as well as CO_2 measurements are planned for the transistion quarter and FY 1977
• DF data should be obtained for a wider range of climatic conditions and geographic locations	• High-resolution 3-to-5-μm spectra in addition to additional fixed-frequency DF data will be obtained in the Chesapeake Bay area during the transition quarter and at another site (possibly Cape Canaveral AFS) during FY 1977
• Experimentally confirmed models and algorithms should be developed for laser propagation at the three major wavelength regions (CO_2, DF, CO) for the canonical sea-level conditions	• The NRL field data used in conjunction with backup laboratory measurements directly tackle this problem

• The above should be repeated for broadband high-resolution FTS transmission	• The NRL SMI system will provide data for comparison to modeling predictions using the NRL in-house code with updated line parameters derived as appropriate from supporting laboratory data

Aerosols

• Total-extinction and angular-scattering measurements should be performed at a large number of geographical locations for a wide range of climatic conditions	• Total extinction will be measured with FTS and fixed-frequency techniques, supported by aerosol-distribution and refractive-index measurements
• The atmospheric character should be monitored simultaneously with field measurements	• This is historically a strong point of the NRL field-measurement program
• High-resolution FTS instrumentation should be made available for broadband field extinction measurements	• The NRL SMI system will be in the field during the transition quarter and FY 1977.

The NRL field-measurement program directly responds to the PSP recommendations as set forth in their report. The experience of the NRL field-measurement team and the unique facilities which they have developed for long-path atmospheric transmission measurements combine to offer a host of compelling arguments for the execution of the planned program.

6. FIELD-EXPERIMENT TEST PLAN

To meet the program objectives set forth in the preceding sections, a continuing series of field experiments will need to be planned and executed. This section of the report is an introduction to the appendixes, which deal with the immediate future of the program wherein extended field operations at the Patuxent Naval Air Station are being planned. So that this report will provide a working document that will serve as a reference guide for the instrumentation, experimental procedures, and field operation of the experiment, detailed information is set forth in each of these areas in the appendixes.

7. ACKNOWLEDGMENTS

The authors acknowledge the continued encouragement and programmatical support provided by Drs. D. Finkleman and P. M. Livingston, Naval Sea Systems Command, PM22/PMS-405. Excellent shop support was provided in the construction of most of the mechanical systems described in this report by NRL-CBD machine shop personnel including M. Cochran, M. Denent, J. Cox, and S. King.

The loan of the CW DF laser system by Capt T. Walker, Air Force Weapons Laboratory, is greatly appreciated. The very important help, advice, and contributions of H. Bobitch, TRW Systems Group, in the F_2-gas-supply-system design, initial DF laser operation and subsequent design improvement, and in many additional ways is highly valued and greatly appreciated.

8. REFERENCES

1. Progress in the NRL experiments carried out at NESTEF, Webster Field, St. Inigoes, Md., was reported in unclassified appendixes consistently titled "The Propagation of Focused Laser Beam Through Near-Earth Atmospheric Turbulence" which have appeared in several NRL High-Energy-Laser-Program Progress Reports during 1970 through 1972. These Secret reports are the following:

Reporting Period	NRL Memorandum Report Number	Report Publication Date
1 July 1970-15 Oct. 1970	2197	14 Jan. 1971
15 Oct. 1970-15 Jan. 1971	2222	29 Mar. 1971
15 Jan. 1971-15 Apr. 1971	2274	11 June 1971
15 Apr. 1971-15 July 1971	2349	22 Oct. 1971
15 July 1971-15 Oct. 1971	2382	17 Jan. 1972
15 Oct. 1971-15 Jan. 1972	2421	18 Apr. 1972
15 Jan. 1972-15 Apr. 1972	2453	30 June 1972

2. H. Shenker, J. A. Dowling, and J. A. Curcio, "Propagation of Focused Laser Beams", Proceedings of the Technical Program, Electro-Optical Systems Design Conference-1971 West, Anaheim, California, 18-20 May 1971.

3. J. A. Dowling and P. M. Livingston, "Behavior of Focused Beams in Atmospheric Turbulence: Measurements and Comments on the Theory," *J. Opt. Soc. Am.* 63, 846 (1973).

4. J. A. Dowling and P. M. Livingston, "Atmospheric Extinction Measurements for Several DF Laser Lines Near 3.8 μm," paper IV-3, VI International Laser Radar Conference, 3-6 Sept. 1974, Sendai, Japan.

5. J. A. Dowling, "Naval Research Laboratory Experimental Laser Propagation Research," paper WB1, OSA Topical Meeting on Optical Propagation Through Turbulence, 9-11 July 1974, University of Colorado, Boulder, Colorado.

6. J. A. Dowling, "The Effects of Atmosphere Turbulence on High-Power Laser Propagation," guest article in the Journal of Defense Research, Series 7B, Number 1, 335-345 (Spring 1975.)

7. R. A. McClatchey and J. E. A. Selby, "Atmospheric Attenuation of DF Laser Radiation," Cambridge Research Laboratory report AFCRL-72-0312, 23 May 1972.

8. R. K. Long, F. S. Mills, and G. L. Trusty, "Calculated Absorption Coefficients for DF Laser Frequencies," Ohio State University Electroscience Laboratory Report prepared on contract F30602-72-C-0016 for Rome Air Development Center, report RADC-TR-73-389, Nov. 1973.

9. D. J. Spencer, G. C. Denault, and H. H. Takimoto, "Atmospheric Gas Absorption at DF Laser Wavelengths," *Appl. Optics* 13, 2855-2868 (Dec. 1974).

10. J. H. McCoy, D. B. Rensch, and R. K. Long, *Appl. Optics* 8, 1471 (1969).

11. R. E. Roberts, J. E. A. Selby, and L. M. Biberman, "Infrared Continuum Absorption by Atmospheric Water Vapor in the 8-12-μm Window," *Appl. Optics* 15, 2085-2090 (Sept. 1976).

12. D. E. Burch, E. B. Singleton, and D. Williams, *Appl. Optics* 1, 359 (1962).

13. R. A. McClatchey, "Atmospheric Attenuation of CO Laser Radiation," Cambridge Research Laboratory report AFCRL-71-0370, 1 July 1971.

14. R. K. Long and F. S. Mills, "Calculated Absorption Coefficients For Low-Vibrational CO Laser Lines," Ohio State University Electroscience Lab. Report prepared under contract F30602-72-C-0016 for Rome Air Development Center, report RADC-TR-74-95, Mar. 1974.

15. J. H. Taylor and H. W. Yates, *J. Opt. Soc. Am.* 47, 223 (1957).

16. R. E. Meredith et al., "Investigations in Support of High Energy Laser Technology, Volume I: Measured Molecular Absorption Line Parameters for CO_2 at 10.4 μm and Anomalous Parameters for H_2O at 0.93 μm and 10-14 μm," Final Report on contract DAAHO1-73-C-0786 prepared for the Defense Advanced Research Projects Agency/STO by Science Applications Inc. Ann Arbor Michigan, SAI Report SAI-75-001-AA.

Appendix A

PLANNED MEASUREMENT LOCATION

The location selected for a series of propagation tests beginning in September 1976 is along the western shore of the Chesapeake Bay directly south of the mouth of the Patuxent River. Two alternate paths have been identified using the three sites shown in Fig. A1. All sites are located on the property of the Patuxent River Naval Air Station. Sites designated A and B will serve as alternate transmitter sites, with C being used for the receiver. Path AC is 6.9 km and will be used for measurements of low absorption (DF and a few low vibrational CO lines); path BC is 5.1 km and will be used for CO and CO_2 measurements.

Several trailers house the equipment used in the experiments to be described in detail in subsequent appendixes. Generators have been used in previous experiments; however it is anticipated that station power will be available at each of the three sites, precluding the need for generator power.

This location has been selected for a continuing measurement program as the best compromise location satisfying the following constraints:

- The location offers controlled access, with all sites on DoD property;

- The overwater path, although not necessarily representative of open-ocean maritime conditions, will afford low-turbulence and clear-line-of-sight conditions;

- The location is within commuting distance for all of the personnel associated with the experiment, making it feasible to conduct continuing operations over several months without major personnel hardship or significant impact on travel funds;

- Any major experimental modifications requiring transportation of a trailer to NRL will result in minimal inconvenience to the operating schedule and nominal transportation costs.

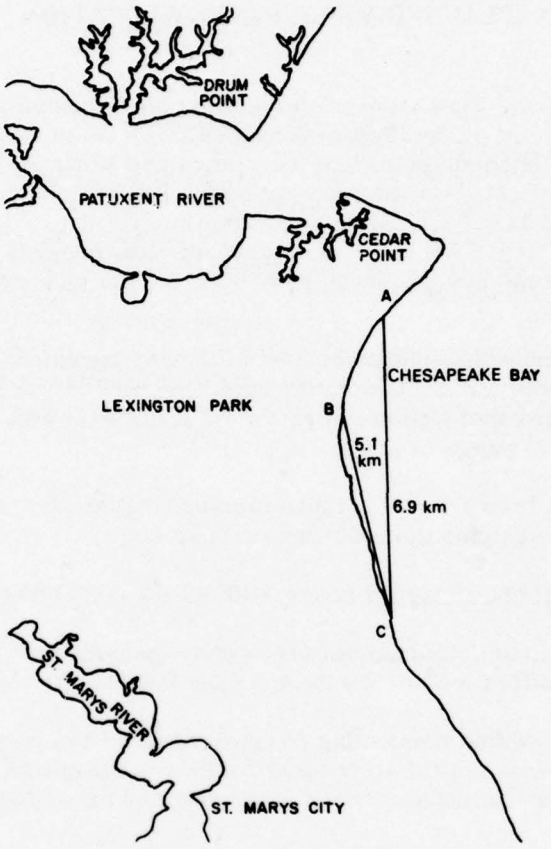

Fig. A1—Atmospheric-propagation-measurement sites at the Patuxent Naval Air Station: (A) transmitter site for a 6.9-km path, (B) transmitter site for a 5.1-km path, and (C) receiver site

Appendix B

EXPERIMENTAL PROCEDURES

B1. LASER-RADIATION EXTINCTION MEASUREMENT

The configuration of the trailers used in the measurement of long-path (≈5-km) optical extinction is shown in Fig. B1. The receiver trailer is normally at the opposite end of the ≈5-km path from the transmitter trailer and associated equipment. Every several days during the course of a measurement series a zero-path calibration is carried out, with the receiver trailer placed as shown by the dotted outline in Fig. B1. A schematic diagram of the optical and electrical signal flow in the experiment is shown in Fig. B2. A 50% 37-Hz chopper divides the laser beam into reference and long-path-measurement components. The long-path information is then transmitted over the path parallel to the measurement beam by use of a data link based on a GaAs laser and a diode.

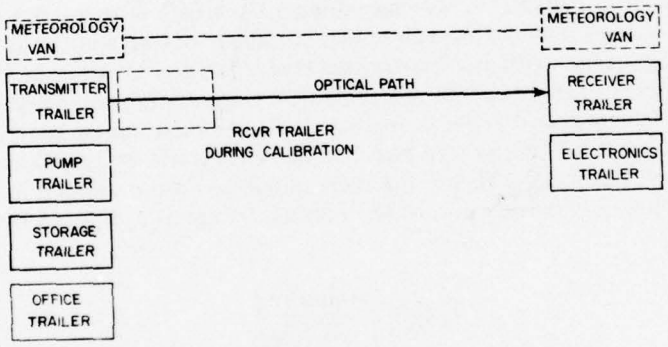

Fig. B1—Trailer locations of the atmospheric propagation measurements

B2. OPTICAL CALIBRATIONS

The measurements of long-path atmospheric laser-radiation extinction involve three basic steps. First the response of a stationary (reference) detector relative to that of a mobile (receiver) detector is determined at each laser frequency to be studied under long path conditions. The mobile detector is placed at the position labeled CAL. in Fig. B2. The mobile-detector preamplifier output is connected to a voltage-controlled oscillator (VCO), which in turn is connected to a frequency-to-voltage converter (FVC). All instrumentation including the ratiometer is contained within the transmitter trailer (Fig. B1) for this measurement. This measurement is conventionally referred to as either an A run (prior to a long-path measurement) or a C run (after a long-path measurement).

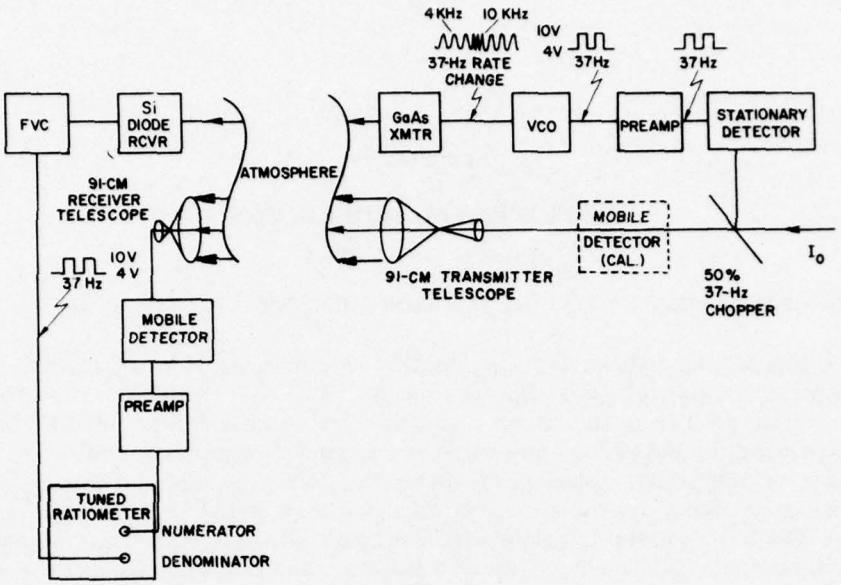

Fig. B2—Schematic diagram of extinction measurements

The second step in calibrating the measurement consists in using the configuration as shown in Fig. B2 except that the measurement is carried out at zero path with the receiver trailer directly in line with the transmitter trailer (dotted location in Fig. B1). In this way the combined reflectivity of three mirrors in the transmitter trailer beyond the chopper plus two mirrors in the receiver trailer is measured. This measurement is normally referred to as a B run, and here it is done at zero path. If the signal ratio at a particular wavelength λ_i measured in the A run is $R_A(\lambda_i)$, and the corresponding ratio measured in the zero-path B run is $R_{B0}(\lambda_i)$, then the transmission of the optical system at λ_i is given by

$$T_o(\lambda_i) = \frac{R_{B0}(\lambda_i)}{R_A(\lambda_i)}. \tag{B-1}$$

Each time a measurement is made, a variable attenuator incorporated into each detector preamplifier is set so as to keep the denominator signal into the ratiometer less than 4 volts peak to peak and also to keep the measured ratio near unity. The 12 attenuator steps numbered 1 through 12 with increasing gain have gain steps to $10^{1/4}$ accurate to 0.01%. Therefore the true ratio of detector signals R_A is obtained from the observed ration R'_A with arbitrary gain settings according to the relation

$$R_A = 10^{(G_M - G_s)/4} R'_A, \tag{B-2}$$

where G_M is the numerical value of the mobile-detector preamplifier attenuator setting, G_S is the corresponding quantity for the stationary-detector preamplifier, and R_A is the observed ratio of the mobile-detector signal to the stationary-detector signal.

The third step in performing the extinction measurements is to record a B run at long path for each of the frequencies to be measured. The long-path transmission at λ_i is then obtained from the relationship

$$T(\lambda_i) = \frac{R_B(\lambda_i)}{R_A(\lambda_i)T_o(\lambda_i)} . \tag{B3}$$

The values of R_A are checked before and after the R_B measurements, and $T_o(\lambda_i)$ is measured every several days during the course of an experiment, since this measurement involves moving and repositioning the receiver trailer.

Figure B3 shows plots of the ratios R_A and R_C versus wavenumber for a typical run made during the Florida DF experiment. The curves shown in the figure are least-square fits to individual data points, and the curve-fit values are used in Eq. (B3) to derive the transmission for each line. Constancy of the ratios R_A and R_C over a day such as shown in Fig. B-3 demonstrate that reliable operation of the measurement system is being obtained.

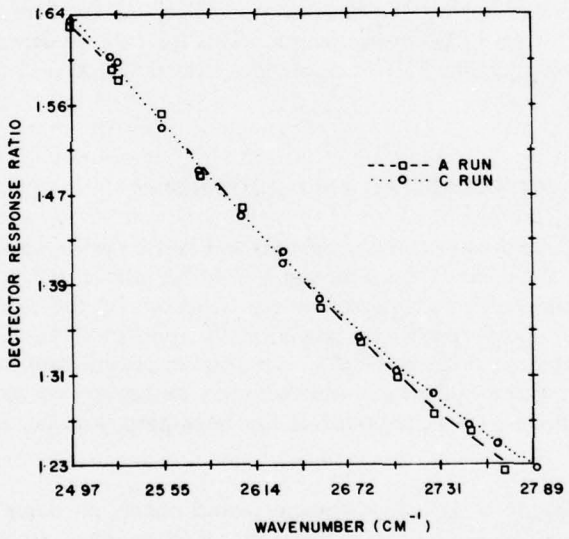

Fig. B3—Typical detector relative-response data obtained in the Florida measurements in 1975

B3. SCANNING-MICHELSON-INTERFEROMETER MEASUREMENTS

A graybody source (described in Section C1 of Appendix C) is used in place of the lasers as a source for the scanning Michelson interferometer (SMI). The graybody source will be imaged at the focal point of the 91-cm Cassegrainian telescope, which will then project a beam over the measurement path. The graybody-source beam will be approximately 4 m in diameter at 5 km using the transmitter collimating telescope. It is calculated that the collimation achieved with transmitter optical system in combination with the 120-cm receiver collecting mirror will allow the use of a relatively modest graybody source (1400-K, 50-W SiC element) without serious problems due to insufficient signal level. Reference spectra for background normalization will be obtained by taking spectra with the interferometer while the graybody source is shuttered. Absolute transmission calibrations for the high-resolution interferometer spectra will be obtained by laser-radiation extinction measurements described in the previous section. Additional details regarding the operational procedure for the SMI instrument can be found in Section C3 of Appendix C. It is anticipated that high-resolution spectra will be taken periodically throughout the interval devoted to transmission measurements on a given set of laser lines (approximately 90 minutes is required to perform a transmission measurement for the 22 DF lines used in the Florida and California experiment). A 5-to-10-minute interval should be sufficient to co-add enough interferograms from the SMI scanning at 20 to 30 seconds for a full scan, such that good signal/noise ratios are achieved in the averaged interferogram prior to transformation. Using the Carson Systems data system and hard-wire fast-Fourier-transform (FFT) processor, a 1.3-to-6.0-μm, 0.0625-cm^{-1}-resolution spectrum should be obtained by Fourier transformation of the averaged interferogram in approximately 10 minutes of processing time. This operation corresponds to a 250,000-point double-precision (32-bit) FFT and includes interpolation and phase-correction operations.

B4. GAS-FILTER-SPECTROMETER MEASUREMENTS

The gas-filter-spectrometer (GFCS) system will be located as shown in Sections C2 and C4 of Appendix C. By means of a relocatable folding mirror and transfer optics the radiation from the transmitter graybody source collected by the 120-cm receiver collector mirror will be relayed and focused onto the entrance aperture of the GFCS. Since the operation of this instrument lends itself to continuous monitoring, it will be used in one of two modes. During the course of laser-radiation extinction measurements a reading will be taken using the GFCS instrument at the beginning, middle, and end of a run as previously described.

An alternative mode of GFCS operation would consist in using the instrument in a continuous-measurement mode during times that FTS and laser measurements are not being made due to normal maintenance, interruptions, or the like. Diurnal variations in water-vapor concentration would best be studied using this mode of operation in addressing the evaluation of the GFCS as a routine long-path diagnostic device as discussed in Section 5.

Appendix C

INSTRUMENTATION

C1. OPTICAL TRANSMITTER TRAILER

The transmitter facility is a self-contained laboratory housed in a van (Fig. C1). Half of the interior of the trailer is occupied by the transmitter telescope frame and its mount and all of the optics and laser sources are contained within the telescope frame. The other half of the trailer contains electronics, vacuum pumps, gas storage, laser power supplies, communication radios, heaters, storage space, tools, and working space. Mounted beneath the trailer floor are heat exchangers for laser cooling, a fluorine-cylinder enclosure, and a chemical scrubber box. Adjacent to the transmitter trailer is a pump trailer. This trailer houses the large vacuum pump required for the operation of the DF laser. In addition it contains tool storage and workbench facilities. The transmitter optical system, laser sources, and alignment procedures used for extinction measurements over a ≈5-km atmospheric path were reported on at the 1975 Fall OSA meeting* and will be described in the following subsections.

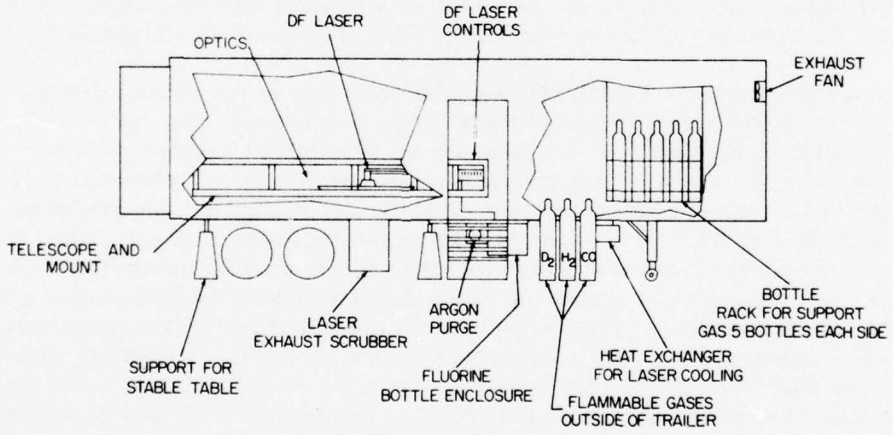

Fig. C1—Layout of the transmitter trailer

*R. F. Horton, J. A. Curcio, and T. H. Cosden, "Optics for a 5-km DF Laser Extinction Experiment," paper ThD 16, 1975 Annual OSA Meeting, Boston, Mass., 21-24 Oct. 1975.

C1.1 Cassegrainian Telescope

The transmitter-telescope optics are shown in Fig. C2. The optics for the 91-cm Cassegrainian telescope were built by Muffoletto Optical Co. The primary mirror (CP) is a 91-cm-diameter cervit parabola with a focal length of 457 cm. The secondary mirror (CS) is a 16.5-cm-diameter hyperbola with approximately a 108-cm convex radius of curvature and is also made of cervit. The telescope has a primary-to-secondary separation of 387 cm, and the system has an effective focal length of 32 m. The focal point f of this system lies 76 cm behind the primary. The optics are gold coated, and the primary is supported by a steel yoke lined with 13-mm-thick felt. Minor-adjustment means are provided for positioning the primary mirror (CP). In transit it is held captive by additional steel supports bolted onto the mount prior to shipment.

The hyperbolic secondary mirror (CS) is held in position by a cross-shaped spider support (Fig. C2) with vanes 6.3 mm thick. Adjustments for positioning and translation of the secondary mirror along the optic axis of the telescope are provided. A coarse-focusing adjustment of the system is provided by this translation, since changing the primary-to-secondary separation changes the effective focal length of the system.

Light coming from either a laser source or the broadband source is brought to focus at the focal point of the Cassegrainian system by an off-axis parabola (OAP) and flat mirror (F1). A 0.25-mm aperture is at the focal point of the off-axis parabola for alignment. It is fastened to a pivoted mounting so that after it is removed for measurements, it can be replaced exactly in the same spot when necessary for later alignment.

The off-axis parabola (OAP), flat mirror F1, and focal-point aperture (RP) along with an entrance-pupil mask (M) are mounted on a movable platform which can be moved parallel to the optic axis of the mirror (OAP). This allows very fine focusing adjustments.

The flat relay mirrors F2 and F3 allow the optic axis of the off-axis parabola to be folded precisely onto the optic axis of the Cassegrainian system. The focal length of the off-axis parabola is 67 cm. Thus the system is an all-reflecting telescope of about 40 power. The entrance pupil of this telescope is mapped directly onto the exit pupil from the trailer. The reason for the entrance-pupil mask (M) is evident when one notes the positions of the detectors, used in the extinction measurement, as shown in Fig. C3. So that the stationary detector (SD) always sees the amount of radiation that leaves the telescope, the entrance pupil is masked. Since the matching of the laser output power distribution to the telescope entrance pupil is a possible variable in the experiment, the pupil mask eliminates uncertainties which might result from small changes in alignment of the input laser distribution with respect to the telescope axis. Variations in the telescope output beam power caused by the occlusion due to mirror CS and its support and dependence on system alignment are thus avoided.

Figure C4 shows the transmitter telescope mount. The mount provides support for all the transmitter optics and some electronics. The steerable mount rests on the base platform at three points, two bearing/wheel assemblies and a front elevation screw. The front elevation screw (VS) allows fine adjustment of the telescope vertical pointing, and the telescope rotates about the elevation screw on the two wheels (W). Horizontal pointing is accomplished through the adjustment of two screws (S) which locate the rear of the mount. The resolution of both pointing adjustments is sufficient to position the focused spot to within centimeters over a 5-km path.

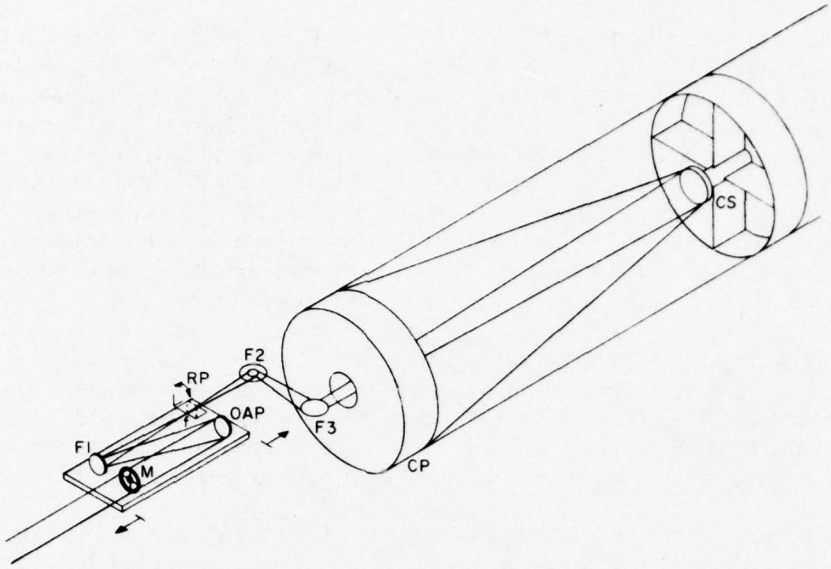

Fig. C2—Cassegrainian telescope: cp = Cassegrainian primary mirror; cs = Cassegrainian secondary mirror; f = focal point; F1, F2, and F3 = flat mirrors; M = entrance-pupil mask; OAP = off-axis parabolic mirror; and RP = removable pinhole

The base platform is supported on four posts which pass through the trailer floor and rest on steel piers, which in turn rest firmly on the ground. Supported in this manner, the mount is decoupled from the body of the trailer and is quite stable.

Two areas of the telescope frame house the laser and the remainder of the optical elements (Figs. C3 and C4). The first area (A in Fig. C4) is between the primary and secondary mirrors below the optical path of the telescope. A DF laser (L3 in Fig. C3) and associated optics and a CO/CO_2 laser (L4) and collimating optics reside here. A periscope-like set of relay mirrors brings output beams from these sources up to the second area.

The second area (B in Fig. C4) is behind the Cassegrainian primary on the level of the fine-focusing lathe carriage and off-axis parabola. In this area the various infrared beams are combined with a HeNe laser beam using beam-combining plates. A final set of relay mirrors match the combined beams to the entrance pupil of the telescope. A Nd-YAG laser and graybody source are also in this area.

C1.2 Laser Sources

The lasers used (other than the GaAs data-link laser) fall into two general categories. Those which are used as laser line sources for actual extinction measurements and those which are used chiefly as alignment light sources. The line sources are DF, Nd-YAG, and CO_2 lasers, and the alignment sources are several HeNe lasers.

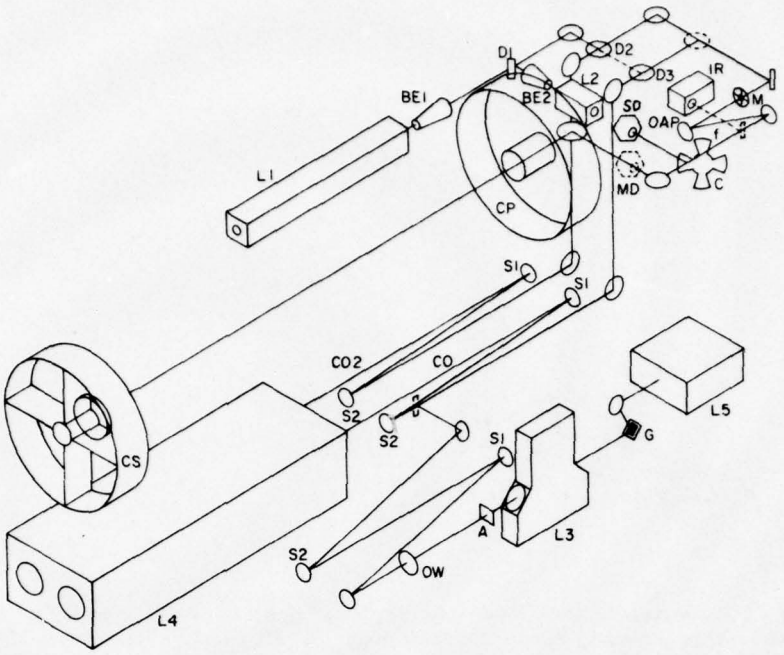

Fig. C3—Transmitter optical system: L1 = Spectra Physics model 125 HeNe laser, BE1 = beam expander and spatial filter, L2 = GTE Sylvania model 605 Nd-Yag laser, BE2 = beam expander and spatial filter, D1 = dichroic beam combining plate (combines 0.6328 μm and 1.06 μm), D2 = dichroic beam combining plate (combines 0.6328 μm, 1.06 μm, and 10.6 μm), D3 = dichroic beam combining plate (combines 0.6328 μm, 1.06 μm, 3.8 μm, and 5.0 μm), IR = gray-body IR source for GFS/SMI, L3 = DF laser, L4 = CO/CO_2 laser, S1 and S2 = spherical mirrors for beam expander, L5 = Lansing VBP HeNe alignment laser, G = grating, A = aperture, OW = output window, C = chopper, SD = stationary detector, MD = mobile detector, M = entrance-pupil mask, OAP = off-axis parabola, f = focal point, CS = Cassegrainian secondary, CP = Cassegrainian primary, and note all unmarked optical elements are flat mirrors

In the 1974 NRL experiments at Cape Canaveral AFS the DF laser used would operate only multiline in the TEM_{00} mode. This necessitated an external monochromator to separate one of about ten individual lines before the radiation was collimated and relayed to the output telescope. In the 1975 Florida and California experiments an improved DF laser with an intracavity grating became available which operated CW with a single-line output in the TEM_{00} mode. Using the second laser, one can select each of the 22 operating lines in turn much more rapidly than the ten lines used with the previous DF laser.

CW DF Laser

The improved DF laser that became available in 1975 and is presently in use was engineered by Mr. Henry Bobitch of TRW Space Systems, Redondo Beach, California.

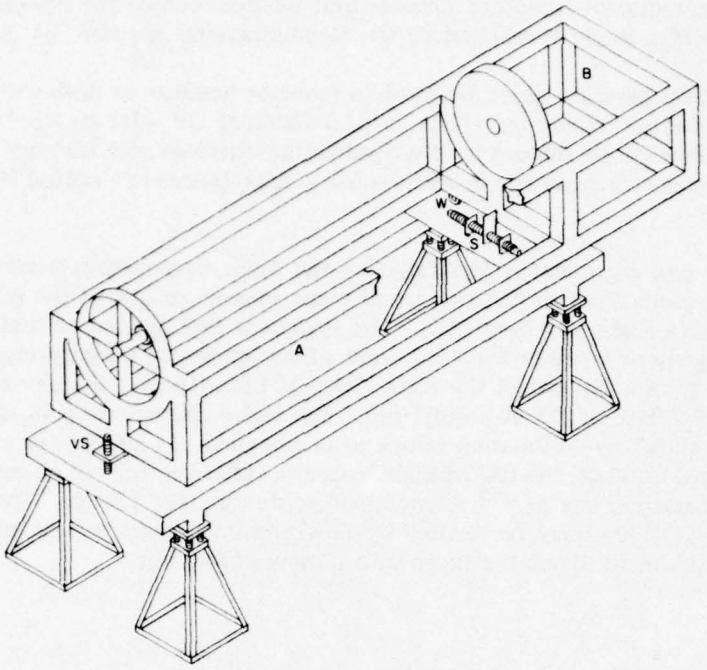

Fig. C4—Transmitter telescope mount: S = horizontal adjustment screw, VS = vertical adjustment screw, W = rollers for horizontal adjustment, B = upper optical bench area, and A = lower optical bench area

The device uses a 15-cm-long linear supersonic nozzle to achieve a gain volume approximately 1 cm square by 15 cm long. This gain volume is situated between two CaF_2 Brewster windows. The long gain path provides approximately a 2.5-W multiline TEM_{00} output, using a gold flat and a 2-m-radius-of-curvature 95%-reflecting output window, or a 0.1-to-0.5-W single-line TEM_{00} output using a J-Y Optical Co. 300-line/mm master grating blazed for 3.75 μm. In either case gas consumption rates are modest. Present cavity fuel-consumption rates have been reduced with respect to the DF laser used originally and are now low enough to allow extended daily operation.

The DF laser and its associated optics are in the telescope frame. As shown in Fig. C3, the laser optical cavity is open. The output window (OW), aperture (A), and grating (G) are mounted along an optical bench. A section of the bench has been cut out to allow the DF laser head (combustion chamber, nozzle, and expansion chamber) to fit through the bench, so that the optic axis of the gain region is in line with the rest of the optical cavity. Adjustments on either end of the laser head allow alignment of the gain region with the axis of the optical cavity. A schematic of the DF laser installation is shown in Fig. C5. In the combustion chamber H_2 is burned in F_2 with a helium diluent at a pressure of 2 torr. The hot gases expand through the linear supersonic nozzle, where D_2 is allowed to react with the disassociated atomic fluorine, forming DF in an excited state. The DF flows between CaF_2 Brewster windows, through the optical cavity where optical power is extracted. The Brewster windows are purged with dry nitrogen to prevent degradation by HF, DF, and F_2. The optical cavity is formed by the grating or flat

mirror and a 2-m-radius-of-curvature ZnSe output window coated for 95% reflectance at 3.8 μm. The TEM_{00} mode is selected by the 2-mm-diameter aperture (A in Fig. C3).

Digital-readout pressure gages are used to monitor pressure in both the combustion chamber and expansion chamber. Gains for the different DF lines may be varied by controlling the flow of He diluent to the combustion chamber and through the throttling of the flow downstream from the nozzles, using a large gate valve located below the laser head.

Calibration and alignment is facilitated by the ZnSe clear output window (OW in Fig. C3), the grating mount, which carries a small plane mirror parallel to the grating, and a Lansing VBP HeNe alignment laser (L5). The system is first aligned so that the reflection of the HeNe alignment beam in the zero order of the grating is a cavity mode; then the grating is set to resonantly reflect the sixth order of 632.818 nm, thereby aligning the grating for the $P_2 8$ line of DF at 3.8007 μm. The HeNe alignment beam and clear ZnSe output window allow the collimating optics to be checked out in rapid succession. Collimation is achieved through the use of high-f-number spherical mirrors S1 and S2. The beam, after collimation, has an e^{-2} diameter of approximately 1.5 cm. The wavelength of the oscillating DF line may be verified by moving an accessory mirror into the collimating mirror system to divert the beam into a monochromator.

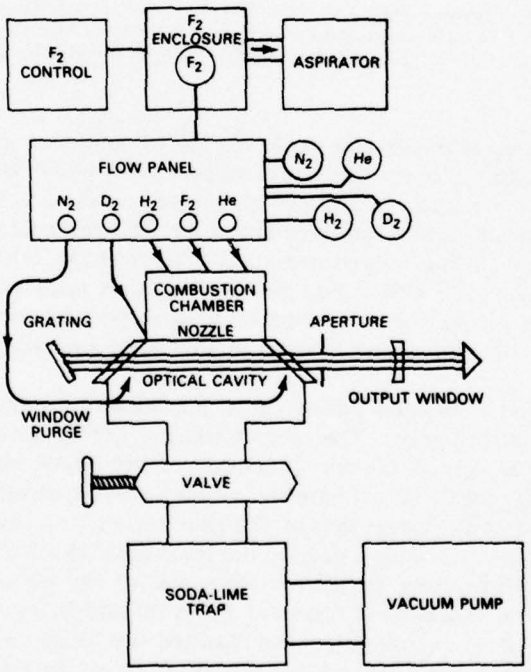

Fig. C5—DF laser

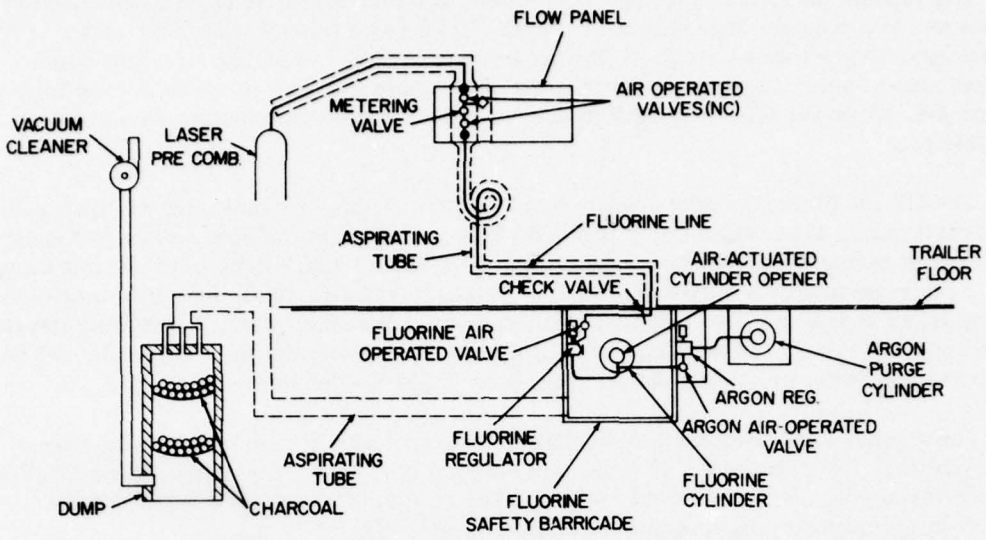

Fig. C6—Fluorine supply system

The fluorine supply system of the DF laser is shown in Fig. C6. Due to the highly reactive nature of F_2 the supply system is isolated from the trailer interior for safety. A standard 2.2-kg F_2 cylinder is located in an aspirated enclosure beneath the floor of the transmitter trailer. The enclosure is aspirated by drawing air through a jacket around the F_2 plumbing in the trailer, through the F_2 enclosure into a carbon bed reactor, and finally into a small vacuum cleaner. The fluorine system uses air-actuated valves controlled from a flow panel inside the transmitter trailer to operate both the flourine and argon supplies.

A second flow panel is used to control the flows of other gases, using both air-actuated valves and manual metering valves. Transducers with digital panel-meter readouts are used to monitor flow rates into the laser. The flow panels and digital readouts are used to monitor flow rates into the laser. The flow panels and digital readouts are fastened to one side of the telescope mount (Fig. C4). Gas lines which connect to the flow panel attached to the telescope frame are flexible enough to allow relative motion between the frame and the trailer body.

Exhaust gases leaving the laser flow through a flexible 15-cm diameter bellows to a chemical scrubber box (soda-lime trap) beneath the trailer. The bellows in the vacuum line allows the relative motion between the telescope frame and the body of the trailer required for pointing the transmitter beam.

The scrubber box (soda-lime trap) is approximately 61 by 61 by 152 cm. (Fig. C7). The laser exhaust gases must flow past the soda lime, contained in six removable trays, which reacts with the HF, DF, and residiual F_2. The remainder of the diluent gases flow to a large vacuum pump through an 2.4-m section of 20-cm-diameter vacuum line installed after the two trailers are located in position.

The vacuum pump is a two-stage 45-m^3/min (750 liter/s) system using a large rotary blower as a low-pressure stage with a 4-m^3/min (70 liter/s) mechanical backing pump. Normal pumping without laser gases flowing and with a "dry" soda-lime trap (one which has had water vapor outgassed), results in an equilibrium pressure of about 80 millitorr in the system. When the laser is operating at normal flow rates, the pressure rises to about 500 millitorr.

The DF gas flow rates were chosen as optimum in trading off laser power output with fuel conservation and vacuum-pump life. The "normal" flow rates chosen allow sufficient laser output power for extinction measurements on all but two of the normally measured lines. For measurements on these lines F_2 and D_2 flow rates are momentarily increased. The system will operate 7 to 8 hours on a cylinder of fluorine (about 2 operating days). Since changing the F_2 bottle takes about 2 hours, F_2 conservation is worthwhile. In addition the soda lime must be changed after every three bottles of fluorine.

The normal flow rates are approximately 2 millimoles/s for fluorine and hydrogen and twice that for deuterium. This gas consumption yields the single-line power distribution shown in Fig. C8, with the exception of the $P_3 9$ and $P_3 10$ lines. These require about 3 millimoles/s of F_2 and about 6 millimoles/s of D_2.

Nd-YAG Laser

The ND-YAG laser is a CW device operating at a wavelength of 1.06 μm. It is used as a source for extinction measurements to allow aerosol extinction to be monitored, since there is virtually no molecular absorption in the atmosphere at this wavelength.

The laser is a GTE Sylvania model 605 laser. It uses a 3-mm-diameter by 63-mm-long Nd-YAG laser rod set in a double-elliptical reflector pumped by two 500-W incandescent lamps. The pumping reflector and YAG rod are water cooled, at approximately 3.8 liters/min. The laser cavity is formed between two dielectric mirrors set in the frame of the device. The output mode is limited to a low order by an aperture in the laser cavity. Output power of the apertured laser is approximately 0.11 W. The mode structure of the laser is further improved during beam expansion through the use of a Tropel Model 280-25 spatially filtered laser collimator which uses a 13-μm pinhole at the focus of a 6-mm-fl lens. The TEM_{00}-mode output power is approximately 80 mW in a smooth-Airy-distribution 2-cm diameter at the collimator output.

Cooling water is provided by a water chiller beneath the transmitter trailer, next to the fluorine enclosure. The chilled water is filtered prior to entering the head to insure unimpeded passage of cooling water through the laser.

The Nd-YAG laser and its spatial filter and collimator are situated directly behind the 91-cm primary mirror, on the optical table which also supports the reference detector. These items are shown in Fig. C3.

Molectron Model C-250 CO/CO_2 Laser

The Molectron laser will be reinstalled in the transmitter. It will be located in the region beneath the telescope optics along with the DF laser. The CO output beam will

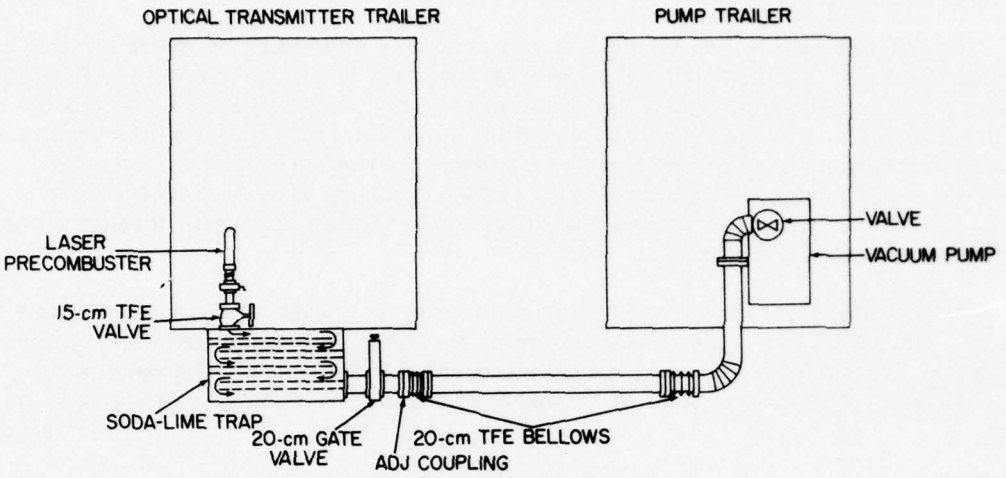

Fig. C7—Vacuum system

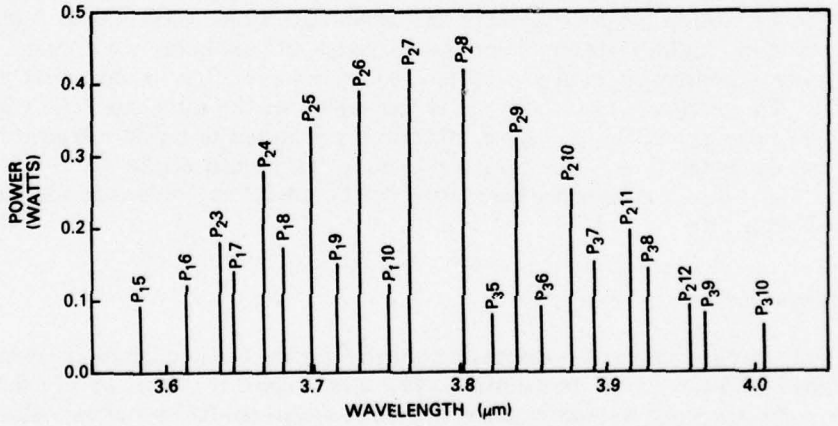

Fig. C8—Power spectrum of the DF laser

share the telescope optical train with the DF laser. The Molectron CO_2 laser is an electrical discharge laser using a 1.5-m-long cavity with a curved output window and a sinusoidal-drive grating for line selection. The laser cavity is apertured to develop a nearly TEM_{00} mode structure. Laser output power is greater than 0.5 W for the P6 through P46 lines in the 10.6-μm band of CO_2.

The CO_2 laser beam is collimated to approximately a 25-mm $1/e^2$ diameter using an off-axis system of high-f number spherical reflectors (Fig. C3). The laser-supply CO_2 gas cylinders line the left front side of the transmitter trailer, and the gas-flow controls are on the laser head. The laser power supply is on the left side of the transmitter trailer, with the discharge-current and voltage meters within easy viewing of the laser operator. The flow of discharge gases is produced by a 16-liter/s pump in the extreme left corner of the trailer. Cooling water for the Molectron and DF laser is circulated through a heat exchanger beneath the trailer.

The Molectron CO laser uses flowing liquid nitrogen to sufficiently cool a mixture of CO, O_2, He, and N_2 to produce laser action on the higher vibrational bands of the CO spectrum. The discharge tube and optical accouterments are basically the same as for the CO_2 laser. The same vacuum pump, gas flow panel, and discharge power supply are used.

The CO laser has been used only a few times, concentrating on the region near 5.0 μm where the atmospheric window will allow extinction measurements. Although the calibration is somewhat uncertain, 16 lines have been observed between 5.00 and 5.20 μm.

Low-Vibrational-Transition CO Laser

Current planning includes the procurement of a low-vibrational-transition CO laser to be used for extinction measurements in the wavelength range form 4.8 to 5.2 μm, where conventional liquid-nitrogen-cooled gas-discharge CO lasers do not operate. Xenon (which is rather expensive) is used as a diluent for reasons relating to molecular momentum transfer. The discharge electrodes are in the region of the discharge tube which is liquid-nitrogen cooled, and the lasing gas mixture is precooled in liquid nitrogen before it flows into the discharge tube. The helium diluent is introduced at the warm ends of the tube. It is planned that this laser discharge tube will be interchangeable with the Molectron laser CO discharge tube.

HeNe Alignment Lasers

The final laser sources worth discussing are the several HeNe alignment lasers required for the operation of the transmitter. The main alignment laser, to which both the transmitter and ultimately the receiver are aligned is a Spectra-Physics Model 125 laser. This laser develops approximately a 75-mW output in a "TEM_{00}-like" mode. Because this laser is being used for collimation through the Cassegrainian system, the laser output is spatially filtered and collimated to a smooth top-hat distribution approximately 2.5 cm in diameter.

Other HeNe alignment lasers include two Lansing VBP lasers. These devices emit a narrow HeNe laser beam whose direction may be adjusted with respect to a virtual pivot point within about 5°. This pivot point may be positioned in space 0.4 to 1.0 m ahead of the device over a range of about 5 cm both horizontally and vertically. The device is extremely valuable in setting up long-optical-cavity lasers or gratings for lasers.

C1.3 Incoherent Infrared Source

The incorporation of the scanning Michelson interferometer (SMI) and the gas-filter correllation spectrometer (GFCS) requires incoherent radiation to be launched from the transmitter. The source to be used is being supplied by SAI as the source for the GFCS This source (Fig. C9) uses a 1385-K graybody as an IR source. The light from the graybody is focused by folding optics to the focus of the 91-cm Cassegrainian telescope. An internal 750-Hz chopper is provided for modulation for the GFCS. When used as a source for the SMI, the chopper blade will be fixed in a position to pass the radiation. The graybody source will be positioned on the upper optical table such that its output can be relayed to the focus of the output telescope by the insertion of one mirror (Fig. C9).

C2. RECEIVER TRAILER

C2.1 Receiver Optics

The receiver optics collect the transmitted beam after it has traversed the measurement path, and by use of the detector/optical integrator the received intensity is accurately measured. The essential function of the receiver is to collect all of the light and focus it into the detector/integrator.

As shown in Fig. C10, the optics of the receiver system formerly consisted of a 13.3-m-focal-length spherical mirror and auxiliary flat mirrors to fold the beam inside the receiver trailer. The entrance pupil of the collecting mirror was unoccluded. Operating the sphere off axis resulted in minor problems with aberrations, which did not affect the operation of the integrators, as the image size could be 1.3 cm in diameter and still be integrated. Only when the effects of scintillation and beam wander caused the incident beam to wander off of the receiver mirror were problems encountered. For the measurements at TRW-CTS a television camera was used with a beam splitter in the receiver optical train such that the size and position of 1.06-μm spot on the receiver mirror could be monitored from the transmitter trailer using a TV picture and microwave relay link.

With the addition of the scanning Michelson interferometer the receiver optical requirements become more severe. The system must furnish a 5-cm pupil for the SMI. Optics with quarter-wave accuracy will be maintained up to the SMI, so that no further modifications will be needed for possible future use of the SMI and a source in the receiver trailer as a stand-alone system.

At the same time, we require the entrance pupil to remain practically unoccluded so as to provide for momentary changeover between SMI operation and laser-radiation extinction measurements. In addition it is desired that the system be used as the collection optics for the GFCS.

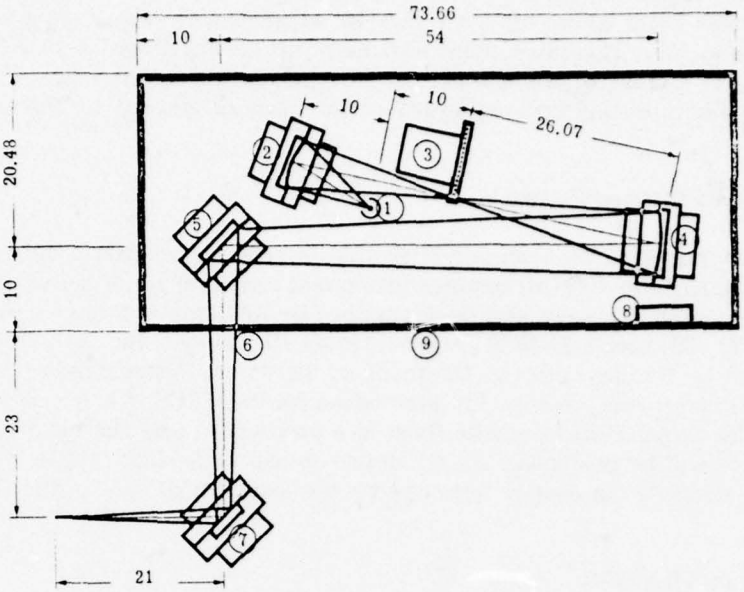

Fig. C9—Graybody source (dimension in centimeters): (1) source element, (2) 5-cm-diameter 6.7-cm-focal length spherical mirror, (3) 750 Hz chopper, (4) 5-cm-diameter 21-cm-focal-length spherical mirror, (5) 5-cm-diameter flat mirror, (6) 2.5-cm-diameter exit port (7) 5-cm-diameter flat mirror, (8) power switch, and (9) cover and base

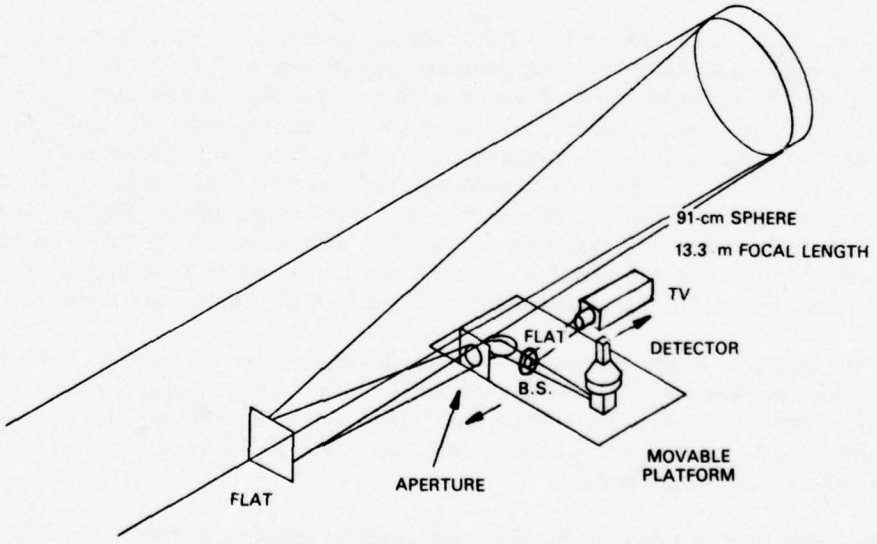

Fig. C10—Receiver optics for extinction measurements

The NRL atmospheric measurements program recently obtained a 120-cm-diameter f/5 parabolic mirror from the Army Ballistic Research Laboratory which is mounted in an optical van trailer. This trailer will be modified so as to be the receiver trailer and house the GFCS and SMI instruments and associated electronics. The 120-cm parabolic mirror offers two significant advantages over the 91-cm sphere formerly used. The first is increased collecting area, thus reducing the effects of turbulence and beam wander. The second advantage is that the parabolic mirror offers $\lambda/6$ performance in conjunction with its use as a collector for the SMI.

The primary disadvantage is that to maintain $\lambda/6$ performance, the 120-cm parabola must be operated on axis. This necessitates a secondary to be located in the entrance pupil of the optical system, occluding the beam.

The solution to this problem will be obtained by using a small Newtonian diagonal and an elliptical relay mirror. The optical system to be used is shown in Fig. C11. The small diagonal mirror (F1) requires the focal point of the system to occur within the entrance pupil of the main collecting mirror (P1). The rays will pass through this focus and then to the ellipse (E) to be refocused outside the entrance pupil of mirror P1. The extinction-measurement detector/integrator will be positioned near this second focus. For SMI or GFCS operation the detector/integrator will be removed and the light recollimated to a 5-cm pupil by a parabolic mirror (P2) for the SMI or GFCS.

C2.2 Optical Layout of the New Receiver

Figures C11 and C12 show the layout of the optical system in the new receiver trailer. Light from the transmitter is collected by the 120-cm parabola (P1), and focused at point f_1. A 1.3-cm-diameter Newtonian flat (F1), is positioned 5 cm ahead of the focus (f_1) of the parabola and reflects the light to an elliptical mirror (E). The ellipse is positioned just outside of the entrance pupil of P1 such that it shares the focal point f_1 with the 120-cm parabola. The second focus (f_2), of the ellipse is on the other side of the entrance pupil. The small parabola (2) has its focus at f_2, and the light is recollimated to the 5-cm pupil needed for the SMI. The 5-cm collimated beam is then sent to an optical table and folded directly into the SMI or alternately folded into the spherical mirror (S1), which provides the necessary image for the GFCS. The extinction-measurement detector/integrator will be inserted in the system near the second focus (D). The mount for this system will be kinematic to allow momentarily changing back and forth between the three modes of operation of the receiver. Further details of the mirrors used in the receiver optical system are as follows:

The primary (P1) is a cervit parabola 122 cm in diameter. The focal length is 6.09 m and the surface accuracy is $\lambda/6$ at 0.5 μm. The mirror is in a mount made by Unertl Optical Co. which is supported on removable piers extending to the ground beneath the receiver trailer. The Newtonian diagonal (F1) will be elliptical, with a 1.3-cm-diameter minor axis. It will be made from cervit 0.67 cm thick. The ellipse (E) will be a 5-cm-thick cervit disk 30 cm in diameter. Major and minor foci will be 71 cm and 234 cm. Only a 14-cm-diameter section of the ellipse will be illuminated; however, because the center of the ellipse will be used for alignment, the ellipse will be left intact. The small

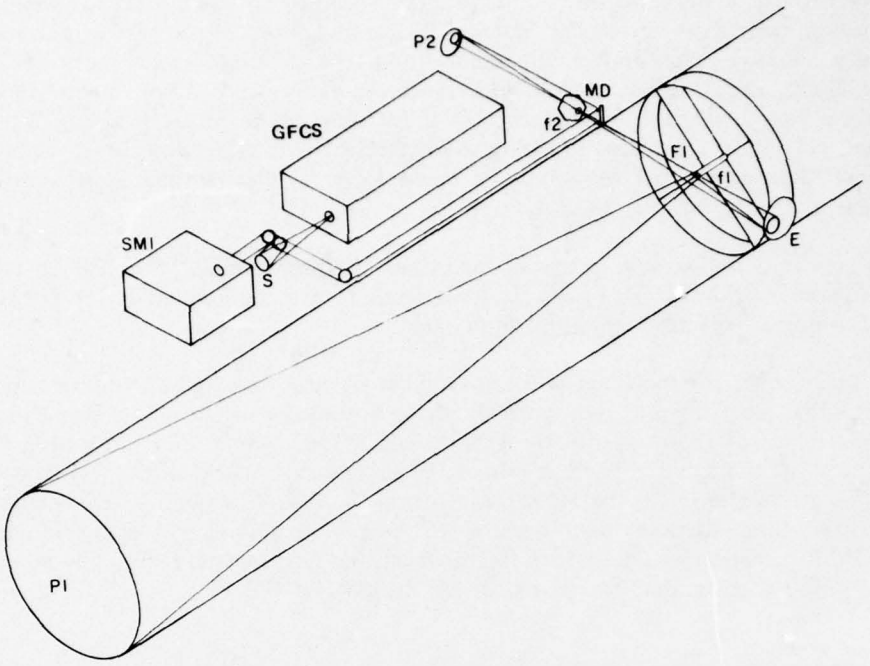

Fig. C11—New receiver optics: P1 = 1.22-m-diameter parabolic mirror with a 6.09-m focal length, F1 = 1.27-cm-diameter Newtonian diagonal mirror, f_1 = focal point of mirror P1, E = elliptical mirror with a 30.5-cm diameter and with f_A = 71 cm and f_B = 234 cm, f_2 = second focal point of the system, P2 = 15.2-cm-diameter parabolic mirror with an 82-cm focal length, MD = mobile detector/integrator in the extinction measurement position, SMI = scanning Michelson interferometer head, S = 66-cm-focal-length spherical mirror, and GFCS = gas filter correlation spectrometer

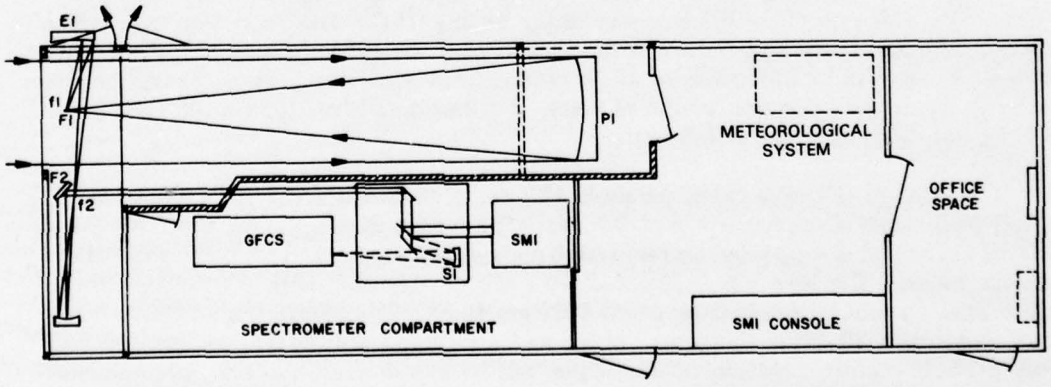

Fig. C12—Receiver trailer floor plan for the new optical system shown in Fig. C11

collimating parabola (P2) will be a 12.7-cm-to-15.2-cm-diameter cervit disk with approximately an 82-cm focal length. The flat F2 will be an elliptical diagonal with a 5.7-cm minor axis. All of these optics will be gold coated to reduce the effects of weathering.

The optical elements will be mounted on a single structure which will combine the elements of a spider support for the Newtonian diagonal F1 in the entrance pupil, a 30-cm-mirror mount for the ellipse, and an optical bench to hold the collimating parabola, the turning flat F2, and the extinction detector. The mount will provide adjustment for all of these elements relative to one another and allow positioning of the entire assembly with respect to the primary mirror (P1). To insure stability, the supports for this assembly will rest on piers.

The layout of the spectrometer compartment is shown in Fig. C12. The locations of the SMI and GFCS are shown. The optical head of the scanning Michelson interferometer will be positioned to allow access through the wall to the FTS data system. A small optical table will hold various beam-handling mirrors and alignment optics. The 5-cm collimated beam will enter the spectrometer compartment parallel to the GFCS. As it is folded onto the optical table, it may be switched to the GFCS by the insertion of a flat into the beam. This is also a logical place for alignment optics and TV-beam-monitoring equipment to watch a HeNe or Nd-YAG reference beam from the transmitter. An optical bench will support the SMI, the GFCS, and the optical table. This bench will be supported through the trailer floor on piers sitting on the ground.

C2.3 Receiver Trailer Modifications

The present status of the receiver trailer requires four major changes or additions:

- An additional 1-m platform is required for holding the spider-and-optical-bench assembly during transit and for providing a comfortable working surface during operation. This platform will have holes in it so that the spider-and-optical-bench assembly may be supported rigidly from piers.

- A cupola which formerly shielded a 30-cm-diameter off-axis turning mirror from the weather must be removed and the door rehung to open outward. The wall at the extreme end of the trailer will have windows installed to allow the 5-cm collimated beam to be transmitted into the trailer.

- The frame and piers which support the receiver optics independently of the body require design and construction. It has been concluded that turbulence-induced beam wander etc. will cause sufficient image enlargement so as to obviate the need for one integrated mount for the entire receiver optical system. Consequently there will be three separate mounts and piers. The present support for the 120-cm primary will be left intact. Mounts and piers will be constructed for the spider-and-optical-bench assembly and the GFCS/SMI optical bench.

- Shelter for the optical components in the field must be provided. Present plans call for enclosing an open area on the deck of the trailer and bringing this enclosure out over a 1-m section which has been added. It is highly desirable to have this enclosure weathertight in the event of storm and to provide for locking the system.

C2.4 Detectors and Integrators

The basic measurement is the ratio of the received power to the transmitted power. The measurement requires two detectors, which produce signals proportional to the total power transmitted or total power received. Figure C13 shows the position of the two detectors in the optical train during measurement and calibration.

Figure C14 shows a schematic of the detector/integrator currently in use. A liquid-nitrogen-cooled InSb bottom-window detector is positioned on top of the integrator. The integrator collects all of the incident radiation, which enters the device horizontally and is folded to the vertical by a gold-coated flat mirror. The integrator consists of four conic aluminum surfaces which have been shot peened. The shot peening produces a rough optically diffusing surface. The center double cone is supported by thin wires and is positioned so that the detector field of view does not include the opposite side of the integrator. A kinematic mount provides consistent positioning.

Figure C15 shows the integrator/detector response to a narrow 1.06-μm beam incident upon the detector for various xy coordinates. The response ideally would show a top-hat distribution which would be independent of wavelength. The InSb detector in use at present is sensitive to a wavelength interval from about 1 to 6 μm. Earlier studies at 10.6-μm using GeAu detectors showed a similar response to that shown in Fig. C15, although the central dimple was slightly more exaggerated.

Presently efforts are being made to improve the detector/integrator assembly. HgCdTe detectors will be used in place of the InSb detectors in order to extend the wavelength response out to 12 μm. The integrator geometry is being studied to see if further improvements can be made. The measured response of an integrating sphere of conventional design is shown in Fig. C16 for comparison.

C3. SCANNING MICHELSON INTERFEROMETER

A scanning Michelson interferometer (SMI) will be used to measure the molecular absorption in the spectral region surrounding each laser line investigated. Since the laser-radiation-extinction experiments determine the absolute atmospheric extinction at each laser frequency, these measurements will be used to normalize the spectral data from the interferometer and thereby to determine the absolute molecular absorption. (Since earlier experiments lacked an interferometer, it was not possible to determine the absolute molecular absorption directly.)

The advantage gained by using an interferometer for making in-the-field spectral measurements in conjunction with the laser-radiation-extinction experiments cannot be overstated. The process of determining the portion of beam loss due to molecular effects also yields the amount of loss due to the nonmolecular effects. At the laser energies involved with these experiments, the nonmolecular effects are generally associated with light scattering from aerosol particles. Thus in the DF region it will be possible to determine the extinction due to aerosols by a direct optical measurement. This determination is also vital to the concurrent efforts to devise a method for predicting aerosol extinction on the basis of Mie scattering theory and the measured size distribution of aerosol particles.

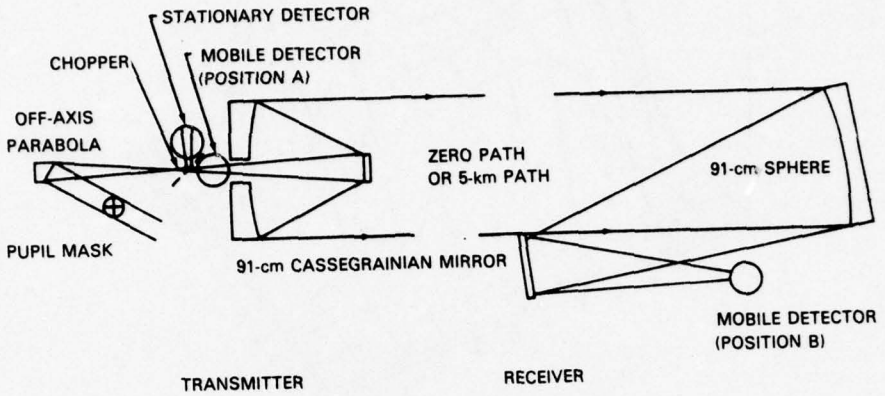

Fig. C13—Extinction measurement scheme

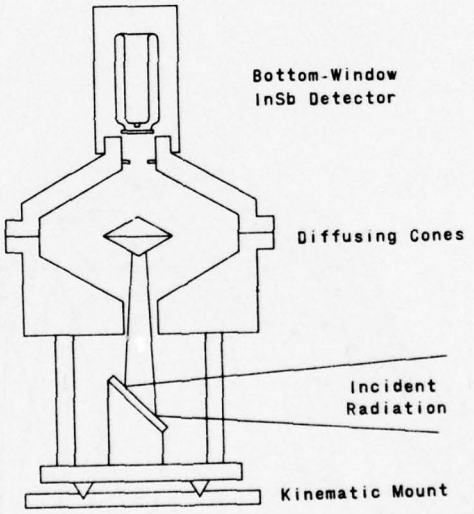

Fig. C14—Present detector/Integrator

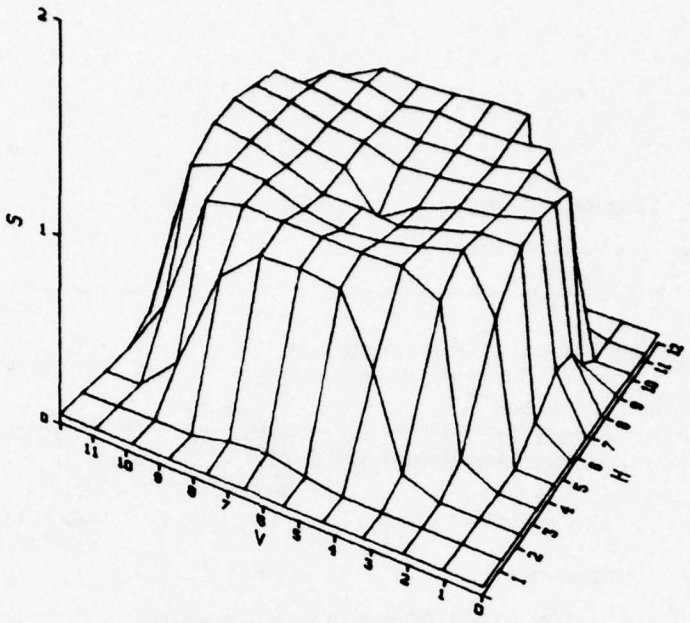

Fig. C15—Spatial response of the present detector/integrator

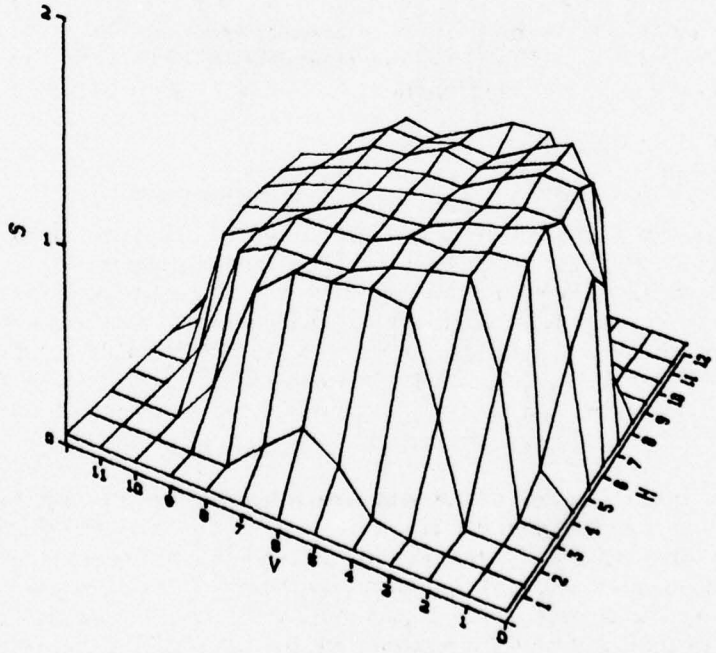

Fig. C16—Spatial response of a detector/integrator with a convential integrating sphere

The continuous-scan Michelson interferometer was selected over other types of instruments because of its high resolution, wide spectral range, wavenumber accuracy, and fast scanning times. (For example the specific device chosen can produce spectra covering the entire region from 2 to 6 μm with 0.06-wave-number resolution in less than 20 min.) Clearly the recent advances in computational techniques and computer hardware have all but eliminated the processing time disadvantage once associated with using interferometers for Fourier transform spectroscopy.

C3.1 Optical System (Interferometer Head)

Figure C17 is a pictorial sketch of the interferometer head, and the optical configuration of the interferometer is diagrammed in Fig. C18. The design is basically that of a Michelson interferometer, with minor modifications to allow the simultaneous use of three separate beams. In addition to the 5-cm-diameter IR beam a HeNe laser reference beam is used to monitor the mirror velocity, and a white-light reference beam is used to locate the moving mirror position at which the path difference is zero. Optical path retardation is variable between 0.016 and 16 cm in eight steps, yielding a maximum spectral resolution of 0.016 cm^{-1}.

The IR signal is recorded by the data system as the moving mirror scans the interferogram. The data system uses the reference signals to begin recording at the zero-path-difference position and to control the mirror velocity (variable from 0.16 to 4 cm/s) during the scan.

The instrument is currently equipped with a CaF_2 beamsplitter and an InSb detector. This beamsplitter/detector combination is particularly well suited for work in the spectral region between 2 and 6 μm. Other available combinations include the KBr beamsplitter and HgCdTe detector, which extends the range to 14 μm.

C3.2 Data System

A block diagram of the data system is shown in Fig. C19. One major function of the data system is controlling the interferometer during the sampling cycle. The system assures proper interferogram positioning and correct sample spacing by monitoring the laser reference signal. A fully automatic mode of operation is also available in which the computer takes over all of the interferometer controls. Additionally the data system continuously monitors the status of critical device components and provides the operator with the diagnostic information needed to maintain the optical alignment of the instrument.

The second major function of the data system is that of processing interferograms to obtain spectra. An interferogram can either be immediately processed or be stored and later combined with subsequent interferograms. (The latter technique is useful in improving the signal-to-noise levels of the output spectra.) The software package contains the routines needed to average, apodize, and transform interferograms and to phase-correct, form ratios of, and plot the resulting spectra. A quick-look low-resolution (0.5-cm^{-1}) spectrum can be displayed on the CRT screen within seconds after sampling has been completed. A transform covering the entire range from 2 to 6 μm with the full

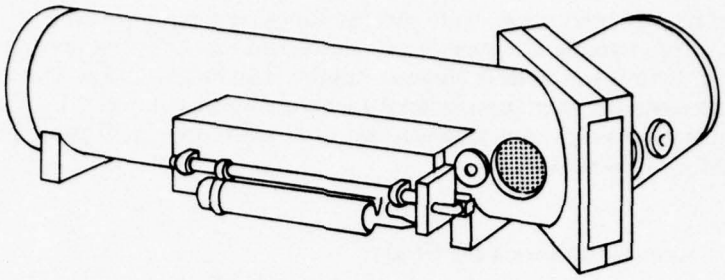

Fig. C17—IDAC-1000 scanning Michelson interferometer head

0.05-cm^{-1} resolution can be processed in less than 10 minutes. The bulk of the processing time is spent performing the Fourier transform. To achieve these extraordinarily short transform times, the system incorporates a specially modified version of the Cooley-Turkey fast-Fourier-transform (FFT) algorithm and uses a hardwired FFT processor (which is attached to the computer as a special input/output peripheral device.)

To maximize the amount of computer core available for data, only a small executive main program is core-resident at all times. The remaining software exists as disk-resident relocatable subroutines which are called into core as needed. Both the data-sampling software and the data-processing software are designed to minimize the operator's interaction with the instrument. In addition the system configuration is designed to provide the type of file-management routines needed to store and manipulate measured spectra.

C4. GAS-FILTER CORRELATION SPECTROMETER

The gas-filter correlation spectrometer (GFCS) is a device using wavelength-dependent absorption by a gas to interrogate the constituency of an unknown atmosphere. The source for the GFCS will be located in the transmitter. The GFCS (being constructed by SAI, Ann Arbor. Michigan) which we will install in the receiver trailer will give us a measure of the atmospheric HDO in a real-world path between the transmitter and receiver vans. Then by use of the established HDO/H_2O abundance ratio of 0.03%, this measurement gives H_2O content along the path.

The GFCS consists of two parts: the filter cell and optics for the actual measurement and the calibration source, which has facilities for a White cell to be placed in the optical system to calibrate system response to the integral of the HDO content over the path.

The GFCS will be accommodated on the front side of the new receiver trailer. Room exists there for both the GFCS and the calibration source. In addition the graybody source in the calibration part of the apparatus may be used as a graybody source for the FTS.

A Perkin-Elmer graybody source is used, operated at 1385 K, focused through a 750-Hz chopper, and coupled into the transmitter telescope. Figure C9 is a drawing of this source. The source output is collimated by the transmitter optical system and traverses the atmospheric path, where part of the radiation is selectively absorbed by the HDO

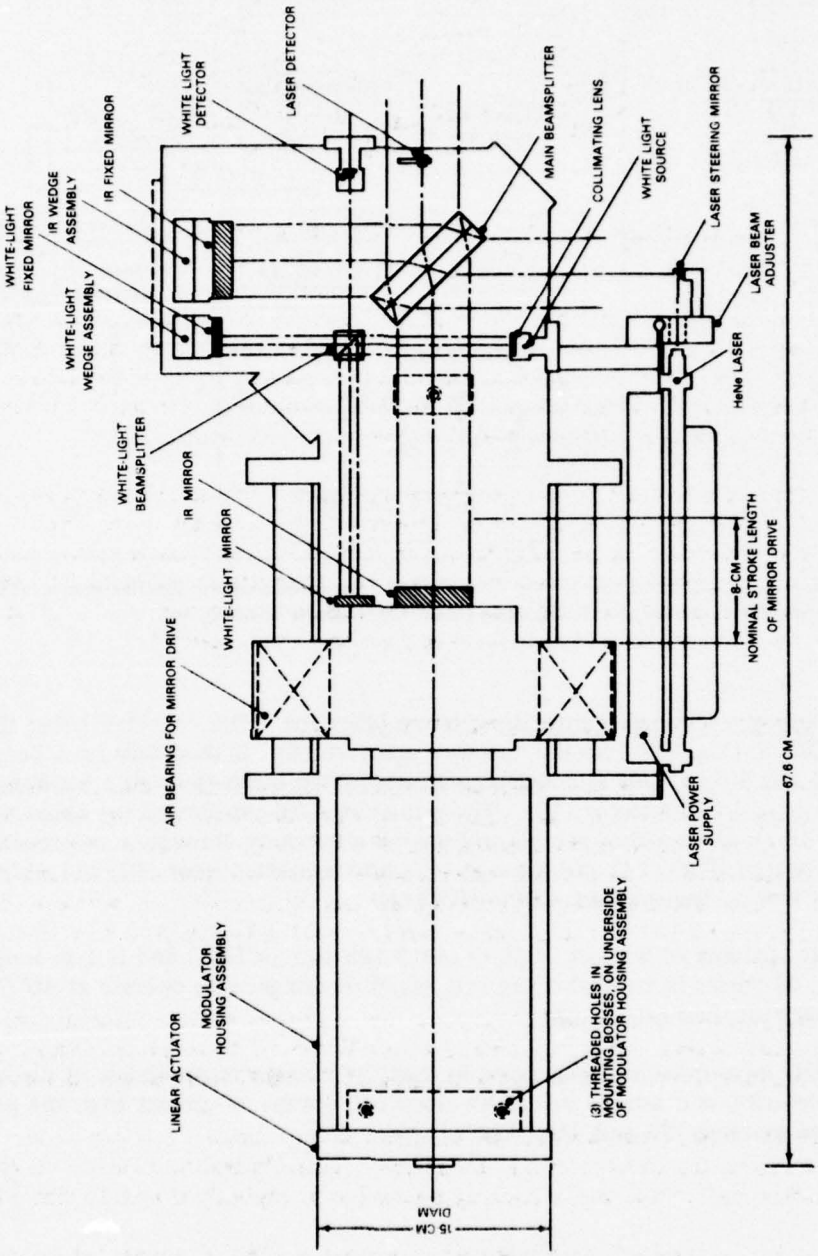

Fig. C18—IDAC-1000 scanning Michelson interferometer

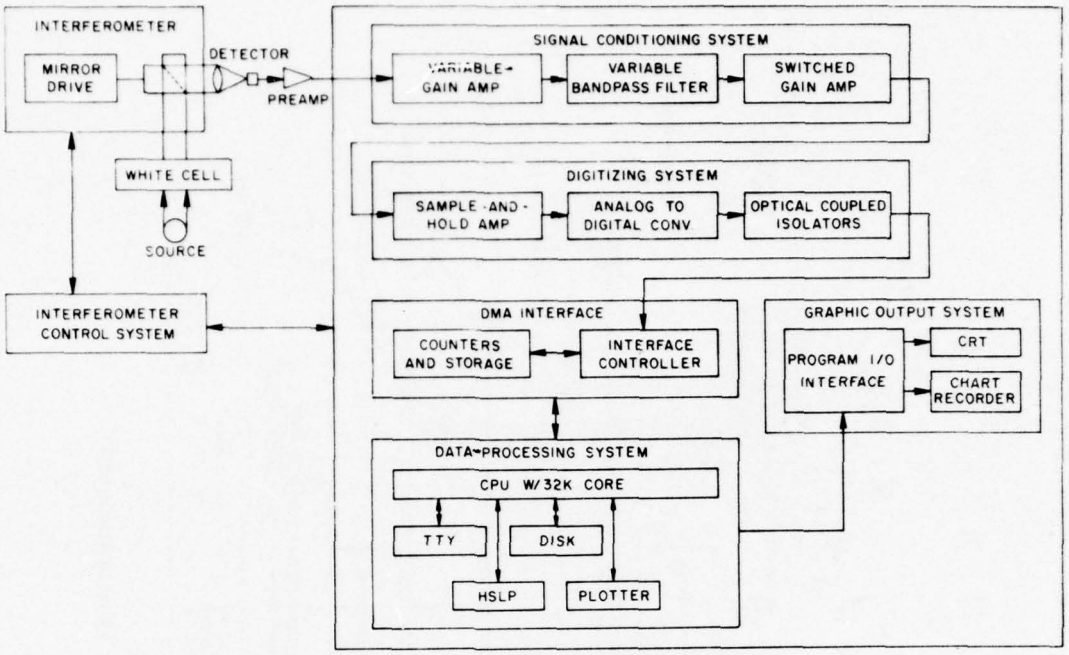

Fig. C19—Functional interconnection of the data-system components of the interferometer. (CPU = Computer Automation LSI-2 central processing unit; HSLP = high-speed line printer.)

constituent and the rest passes into the receiver telescope. The collected beam then enters the GFCS, (Fig. C20) via the entrance aperture (4). It then falls on a beam splitter (7), which sends 40% of this atmospherically attenuated beam through a bandpass filter (18) and onto an InSb detector (19). The remaining 60% portion of the beam is then chopped at 45 Hz by the chopper (8) and passed alternately through a cell containing 100 torr-meters of HDO (14) and through an adjustable attenuator (10, 11) which matches the average transmission of the HDO cell.

The cell contains 31.25 torr of H_2O and 3.125 torr of HDO and is 1 m long. The beam makes 32 passes in traversing the cell, which is designed to operate at 40°C, using a 100-W heater with thermistor control.

The HDO measurement signal arises in that the average transmission of the combination of atmospheric and sample cell HDO (Tac) will always be greater than the product of the individual averages (Ta and Tc). Let

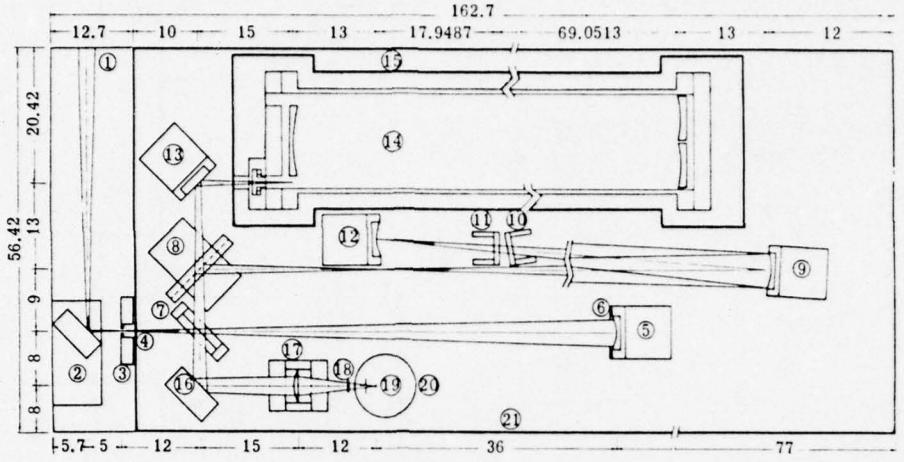

Fig. C20—Gas-filter correlation spectrometer (GFCS) (dimension in centimeters)

$$T_a \equiv \frac{1}{\Delta V}\int_{\Delta V} T_a(V)\,dV,$$

$$T_c \equiv \frac{1}{\Delta V}\int_{\Delta V} T_c(V)\,dV,$$

$$T_{ac} \equiv \frac{1}{\Delta V}\int_{\Delta V} T_a(V)T_c(V)\,dV.$$

Then the measurement signal is given by

$$M = \frac{T_{ac} - T_aT_c}{T_{ac} + T_aT_c}$$

as stated in the design theory of the instrument. During the time when the 45-Hz chopper passes the beam through the reference filter, we have T_aT_c, and for the remaining time, when the beam passes through the HDO cell, we have T_{ac}, so that the signal M appears as a 45-Hz modulation on the detector output.

The reference attenuator is at the virtual pivot of the chopper blade; hence to first order angular wobble in the chopper will not affect the point of intersection on the reference attenuator.

The electronics used to process the various signals are shown in Fig. C21. The detector output goes through a high-gain preamplifier followed by a variable-gain driving amplifier. The signal then passes through a unity-gain bandpass filter tuned to 750 Hz,

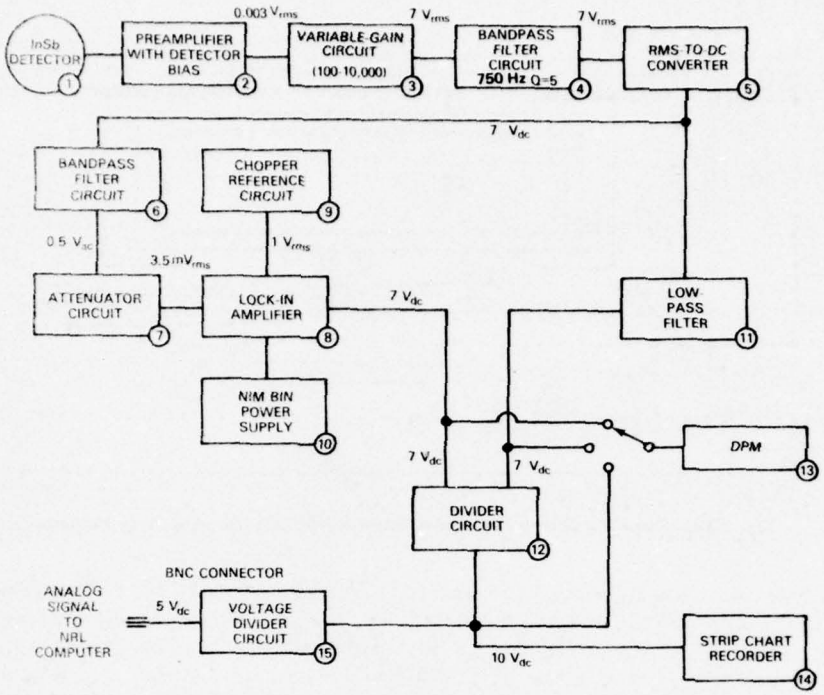

Fig. C21—GFCS electronics. (NIM bin = nuclear instrumentation module housing; DPM = digital panel meter)

after which the signal is rectified. At this point the signal drives two parallel circuits. One is an 0.25-Hz low-pass filter which provides the normalization drive for an analog divider. The second is a unity-gain bandpass filter tuned to 45 Hz followed by an attenuator to provide a 5-mV-level signal for a PAR model 220 lock-in amplifier. An 0.25-Hz time constant is used with the lock-in-amplifier output stage, and the output signal drives the numerator of an analog divider whose output is 10 V dc full scale and drives a digital voltmeter, a strip chart recorder, and an analog-to-digital computer link through a 2:1 voltage divider.

A calibration source (Fig. C22) in the receiver trailer can easily be inserted into the receiver optics train ahead of the GFCS entrance aperture. This source can be operated in two modes. In the first mode there is no HDO in the path; thus the signal can be used to adjust the attenuating neutral-density filter to match the HDO-cell transmission. This adjustment may have to be checked as frequently as every hour of operation.

The second mode of operation is with an HDO cell in place with an adjustable number of passes to simulate atmosphere humidities of from 2 to 20 torr over a path of 5 km. The signal with the cell in place can be used to calibrate the entire system response.

The calibration-source components include a Perkin-Elmer graybody source (1) which is focused by a BaF_2 lens (2) through a 750 Hz chopper (3) and steered through the HDO cell (7) in from 4 to 40 passes. The cell contains 1.07 torr HDO and 10 torr H_2O). The beam is then steered into the entrance aperture of the GFCS.

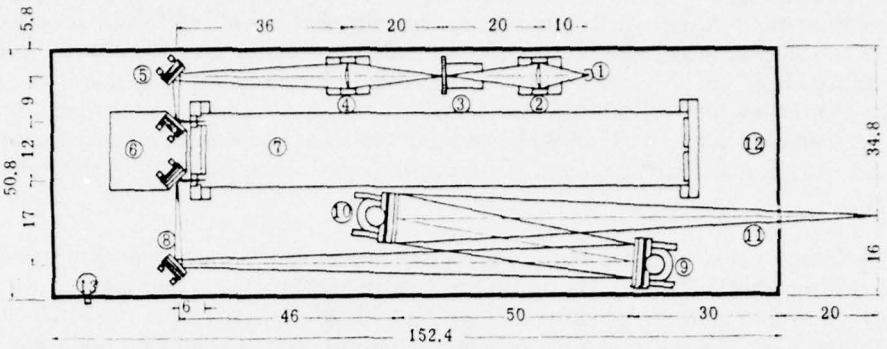

Fig. C22—Calibration source with calibration cell in place (dimensions in centimeters)

C5. ELECTRONIC INSTRUMENTATION FOR EXTINCTION MEASUREMENTS

The electronic instrumentation associated with the scanning Michelson interferometer (SMI) and the gas-filter correlation spectrometer (GFCS) has been described in some detail in the preceding sections and will not be treated in this section. The preamplifiers, optical-data-link modulator/demodulator, and tuned ratiometer used in the extinction measurement procedure (Section B1 of Appendix B) were discussed at the Fall 1975 Annual Meeting of the Optical Society of America* and will be described in this section. The principal components of this system are shown in Fig. B2.

The main goals pursued in the design of this equipment were a ratiometer-system accuracy of 0.2% and ease of use in the field. The system employs optical chopping to eliminate dc drift problems. InSb detector preamplifiers that use current-mode inputs for gain stability were designed so that gain drifts due to the active components are negligible. Reference-channel information is carried on a GaAs optical data link which is sufficiently rugged and stable that its contribution to the error is negligible. The ratiometer comprises precision matched bandpass filters to select the fundamental frequency of the chopped inputs, precision rectifier circuits, a unique dc ratio circuit, and a Bessel filter to average the output. The ratio circuit uses a single logarithmic transistor junction to perform all nonlinear signal operations; hence errors that might otherwise arise from mismatches between several transistors are eliminated. The ratiometer includes a self-calibration feature and automatic-gain ranging to allow a large input dynamic range.

The laser beam is chopped at 37 Hz by a reflective chopper with a duty cycle of 50%. The chopped beam is transmitted by the reflective telescope, propagates through the 5 km of atmosphere, and is completely collected by the second telescope. Two integrating spheres, each with an InSb detector, provide broadband detection of transmitted and received power. Two preamplifiers develop high-level signals representing the optical power transmitted and received. One of these signals is transmitted over an optical data link, and

*R. W. Harris, "Electronic Instrumentation for a High Accuracy Atmospheric Extinction Measurement" paper ThD14, 1975 Annual OSA Meeting, Boston, Mass., 21-24 Oct. 1975.

the two signals are then inputed to a ratiometer which determines the ratio of their 37-Hz spectral components. Although this system is basically a classical two-beam chopped ratiometric transmissometer, its implementation presents some unusual problems due to the large path length and the small value of the expected extinction coefficient to be measured. Careful system calibration and characterization of measurement errors is essential. Transmissions greater than 90% can be observed at some wavelengths; therefore errors in measurements of transmission are magnified tenfold in computing the extinction coefficient.

The ratiometer response is intentionally slow: it has an effective averaging time of 4.3 and a settling time of 17 s. The noise bandwidth (0.086 Hz) is equivalent to a lock-in with the same averaging time. But unlike a lock-in, the ratiometer is insensitive to chopping harmonics; it requires no phase-reference input, and it tolerates moderate drifts in the chopper speed (± 5%).

If the ratiometer were not insensitive to harmonics, the calibration factors of the preamplifiers and data link would be matrices. However with this provision they are scalars. The ratiometer includes automatic-gain-control circuits to cope with moderate changes in the laser intensity. However the AGC does not cause transient errors in the ratiometer output, and this feature is a requirement because of the long settling time. Overall the ratiometer has an error less than 0.2%.

Figure C23 is a block diagram which shows the functional structure of the ratiometer. The ratio detector, in the center, forms the ratio of two dc voltages which come from the ac inputs via two identical channels. The AGC system increments the gains in both channels simultaneously to obtain the best signal levels at the ratio-detector inputs. The output averaging filter provides the slow response. At the input of each channel a bandpass filter rejects harmonics and most of the noise. A programmable-gain amplifier couples the signal to a precision rectifier circuit which produces a virtually exact full-wave rectification. A smoothing filter eliminates the ripple and completes the ac-to-dc conversion, or detection process.

There are several notable features of the ratiometer design. The input filters are well-matched and very stable. The ratio of their gains is independent of frequency and of temperature over certain ranges. The averaging filter is an optimum design which best meets the conflicting requirements of long averaging time versus short settling time.

The ratio detector has a unique design which uses only a single logarithmic element (Fig. C24). The ratio detector contains six switches as shown, which are solid-state devices actuated sequentially by timing circuitry not shown. The four switches on the left are effectively closed one at a time, each with a 25% duty cycle. The other two switches are coordinated with these four; they are effectively closed one at a time with duty cycles of 50% each. Thus four interconnection states in this circuit exist with equiprobable likelihoods. The logarithmic element therefore operates on four voltages. Its output Y is shown as a function of its input X by an equation involving two unknown constants A and B. Since the log element is a transistor used in the transconductance mode, these constants are temperature and age dependent.

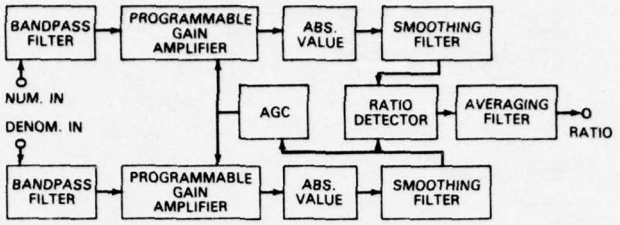

Fig. C23—Tuned ratiometer

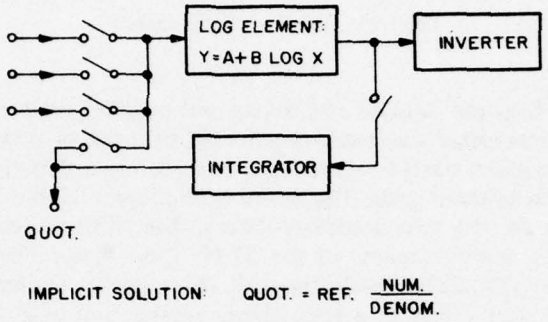

Fig. C24—Ratio detector

The advantage of this circuit structure is that the implicit solution which it obtains is independent of A and B. These parameters simply cancel out due to symmetries inherent in the multiple usage of the one logarithmic element. The reference input is a constant voltage which sets the scale for the output. Its necessity is obvious, since the output has the dimensions of a voltage, whereas the desired ratio is dimensionless. This design provides great accuracy and stability without any fussy adjustments. It was simultaneously and independently developed by the PAR Corporation and by NRL.

The optical-data-link performance characteristics are shown in Fig. C25. The data link is a commercial product of the American Laser Systems Corporation to solve a simple problem in communications. It obviated the need for a microwave link or 5 km of cable. It is small, easy to use, and rugged. It transmits data as a train of optical pulses as shown. The information is entirely contained in the pulse repetition rate or frequency, which varies as shown from 3 to 10 kHz. The pulse amplitudes and durations carry no information. Atmospheric turbulence is therefore no problem unless it causes missing or extra pulses, and this is not a problem. The complete data link is therefore a sort of FM system. Its baseband frequency response is shown here. The chopping frequency lies on a flat portion of the curve.

The optical specifications on the data link are as follows: Both the transmitting and receiving lenses have effective apertures of 3.5 cm. The beam divergence and field of view are 5 milliradians. The optical pulses last 100 ns, peak at 10 W, and are generated by a GaAs laser diode at a wavelength of 0.904 μm. A silicon avalanche photodiode is used for detection.

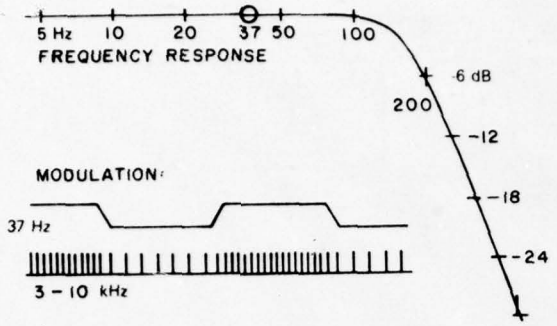

Fig. C25—Data-Link performance

The two preamplifiers are dubbed *stationary* and *mobile*, since one is regularly transported between transmitter and receiver sites for calibration procedures. As shown in Fig. C26, the preamplifiers each contain front ends for two detectors plus a filter and an amplifier with switch-selected gain. The front ends provide stable biasing and stable low-noise amplification for the two detectors inputs. The filter rejects as much noise as possible while preserving the squareness of the 37-Hz waveforms. The frequency response of the filter is shown in Fig. C27. As desired, 37 Hz is on the flattest part of the curve. There are 12 selectable gain values in a logarithmic progression with four steps per decade.

C6. AEROSOL MEASUREMENTS

Any optical equipment which depends on light propagation through an outdoor environment must be designed with a knowledge of the limits imposed on it by the various components of that outdoor environment. The three primary degrading effects on optical propagation in the linear realm are absorption, turbulence, and scattering. The scattering portion is the one which this operation addresses.

Scattering is further divided into that due to molecules and that due to aerosols. In the wavelength region of interest and at atmospheric pressure at ground level the aerosols predominate. (Although the word scattering has been used here in connection with the aerosol problem, extinction is more appropriate, since the transmission losses are due both to scattering and to absorption in the bulk of the individual aerosols.)

Historically the equipment involved in this discussion was gathered and assembled in support of a field laser-transmission measurement, the idea being that transmission is determined by molecular absorption and aerosol extinction. Meteorology instrumentation, including especially the measurement of water-vapor content, was obviously needed for base support for the program. Since the transmission experiments were being done at wavelengths where the transmission was high, the effect of the aerosols on the measurement would not be significant, and at some wavelengths, in the visible for example, it predominates.

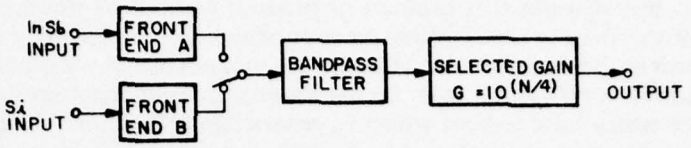

Fig. C26—Detector preamplifier

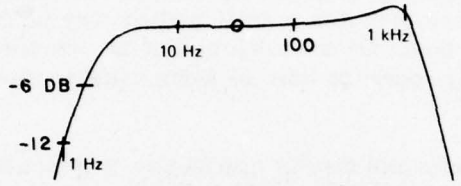

Fig. C27—Frequency response of the detector preamplifiers

Thus a system which could monitor and characterize the ambient aerosols concurrently with the transmission measurements was designed and produced. Since the aerosols are also known to depend on the meteorological variables, it was decided to unite the data-collection efforts of these two investigations. The result was a mobile unit with capabilities for monitoring both the meteorological variables and the aerosols in the vicinity of the unit. This aerosol van is a currently operating system. However it should not be considered a finished product but rather a growing entity, improving with our knowledge of the aerosol measurement problem.

To point out some of the problem areas, we will look briefly at the relationship between the extinction of light and the aerosols. We begin by writing the expression for the linear extinction coefficient σ for a laser beam due to aerosols as

$$\sigma_{\lambda,n} = \int_0^\infty Q(\lambda, n) \frac{dN(r)}{dr} \pi r^2 \, dr, \tag{C1}$$

where λ is the wavelength of light, n is the complex index of refraction of the particles, r is the radius of the particles (assumed spherical, the first hint of problems involved), dN/dr is the aerosol number density distribution, and $Q(\lambda, n)$ is the Mie-theory scattering-efficiency coefficient.

Given the component parts of this expression, it is simple to calculate and thus predict, the optical transmission at a given laser wavelength through a known aerosol distribution made up of particles with a known index of refraction. The obvious deterrent to finding the solution is that most of the components of the expression are not given but must be obtained. This presents many difficult and complicated experimental problems.

The majority of these problems are associated with the complex index of refraction of the particles. For example it is difficult to produce equipment which can make measurements to give the density distribution function which are not strongly sensitive to the index of the particles being measured. Even if the measurements were not sensitive to the index, the problem still exists that the density-distribution function itself is found to describe particles which have indices which in general are a function of size. This relationship is complicated and is found to be different for geographic and general weather variations.

Little is known about the magnitude of this variation of the index as a function of radius for any given distribution. It is known that this variation depends on local conditions. It is also known that even a single particle may be made of an aggregate of particles with different indices. On the other end of the spectrum, for high humidity conditions the aerosol may appear to have an index equal to that of water, which is known quite well.

Figure C28 shows an aerosol density distribution function from the coast of Florida in March 1975. The data were obtained with a Particle Measuring Systems active scattering aerosol spectrometer. This probe sizes and counts particles in the size range 0.1 to 5 μm. The total number density N of the particles in the range described by the curve was 66.6 cm^{-3}, the cross-sectional-area density of those particles was 42.9 $\mu m^2/cm^3$, and as the volume density of the particles was 62.3 $\mu m^3/cm^3$. We will take that distribution, assume that the index is real and does not vary over the size region, and calculate the extinction due to these particles for 3.8-μm radiation.

Equation C1 can be rewritten as

$$\sigma = \int_r Q \, ds, \tag{C2}$$

where ds is the differential cross-sectional area. The two components of the integrand are plotted as a function of r in Fig. C29. Scattering efficiency curves are shown for two indices of refraction. These two values, 1.3 and 1.6, are generally thought to encompass the real portion of the values found in clear air. In Fig. C30 is plotted the running integral over the particle sizes. This is done for four indices of refraction.

Two things are obvious from the last two figures. First, it is important to know the index well, since the resulting extinction calculation for the particles varies by a factor of two. Second, more information must be obtained at the larger particle region, since enough particles are beyond the limit of the probe to still contribute significantly to the integral. This is especially true if the index is nearer to 1.3.

Figures C31 and C32 again shows the running integral for the same particle distribution but for a variation of the imaginary portion of the index. At this wavelength and for this distribution the accuracy of the imaginary portion is not found to be as important as that for the real portion for the extinction calculation. (It would however be more important for thermal-blooming calculations using these data.)

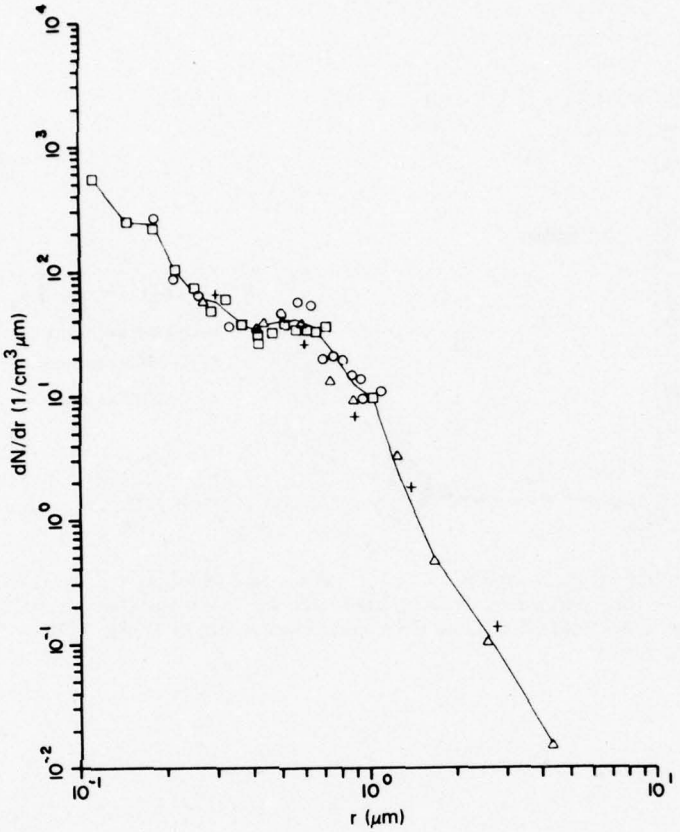

Fig. C28—Aerosol particle size distribution measured at Cape Canaveral Florida, on 19 March 1975 at 1515 hours

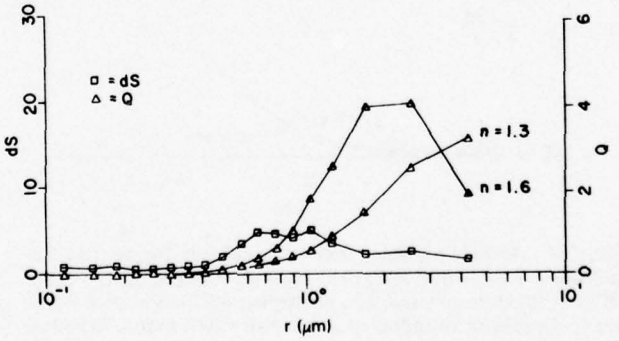

Fig. C29—Aerosol particle cross-sectional area for the particle distribution measured at Cape Canaveral, Florida, on 19 March 1975 at 1515 hours and Mie scattering efficiency at λ = 3.8 μm as a function of refractive index (real part) and aerosol particle size

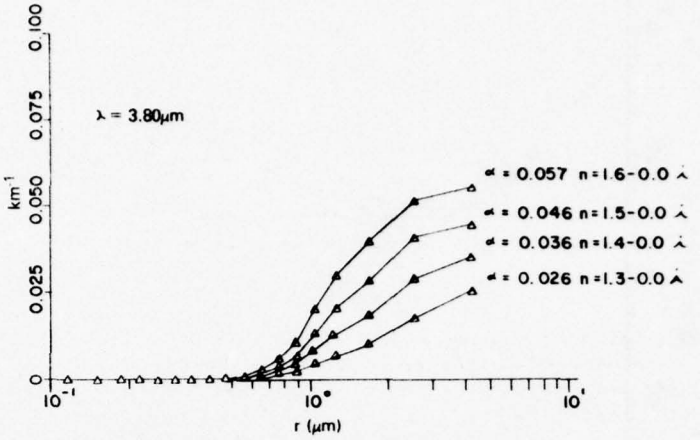

Fig. C30—Optical extinction at $\lambda = 3.8$ μm as a function of refractive index (real part) and aerosol particle size for an aerosol particle distribution measured at Cape Canaveral, Florida, on 19 March 1975 at 1515 hours

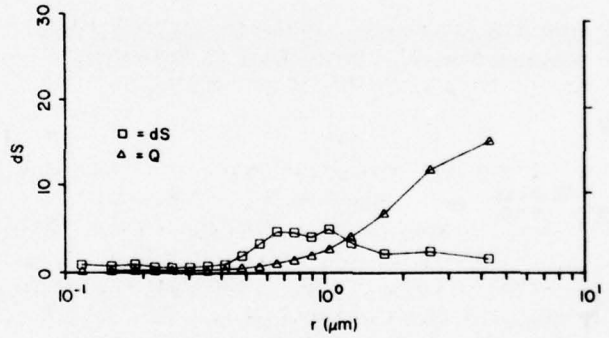

Fig. C31—Aerosol particle cross-sectional area for the particle distribution measured at Cape Canaveral, Florida, on 19 March 1975 at 1515 hours and Mie scattering efficiency at $\lambda = 3.8$ μm for a refractive index of $n = 1.300 - 0.050i$ as a function of aerosol particle size

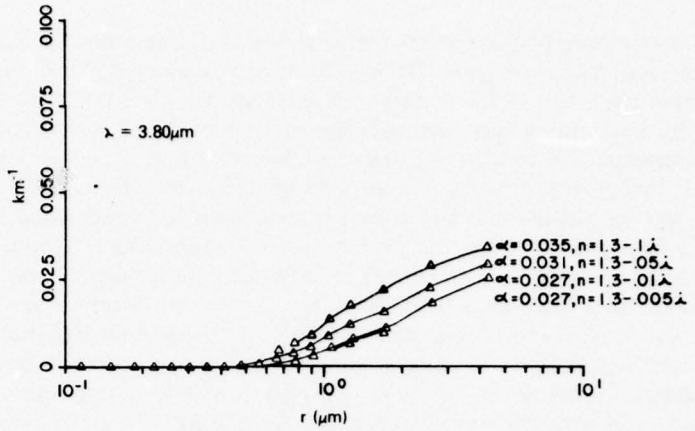

Fig. C32—Optical extinction at $\lambda = 3.8\ \mu m$ as a function of refractive index (imaginary part) and aerosol particle size for an aerosol particle distribution measured at Cape Canaveral, Florida, on 19 March 1975 at 1515 hours

The conclusion is that to be able to successfully predict optical propagation from a point measurement of this type, two technological areas must be developed. One is a method for accurately monitoring the complex index of refraction *in situ*, both as a function of wavelength and as a function of particle size. The other is an approach to sizing and counting the larger particles in a fast way that includes enough particles to be statistically significant but does not modify the particles while sampling. Both of these are extensive research areas and are urgently needed.

In the second area work is underway. A newly designed device is being obtained for this purpose. However it is a state-of-the-art device, and extensive testing will be necessary, both in the laboratory and in the field, before results from its use can be deemed meaningful.

The first area is a difficult one. The initial approach in this operation will be to add a second measurement of the effect of the aerosols which can be compared with the aerosol monitoring equipment through the use of calculational approaches similar to that used in the discussion above. One proposal for this second measurement suggests using a nephelometer which is capable of measuring a volume scattering coefficient at three wavelengths. This measurement, in conjunction with the particle-size distribution currently available, will allow a comparison in a manner which should give more knowledge of the index variation.

Another approach to the index-variation problem would be to devise a system which could separate particles, wet or dry, as a function of size so that an index measurement could be made on the various sizes individually. The caveat here is first due to the wet or dry statement. Even when that problem is solved, the second step is still difficult to do in a manner which does not affect the sample.

C6.1 Active Aerosol-Scattering Spectrometer Probe

The active aerosol-scattering spectrometer probe is diagrammed in Fig. C33. The optics collect the light from a hybrid HeNe laser that is scattered from a particle passing through the sample chamber. This chamber gets its air sample by having the axial blower draw air down the accelerator tube through the sample chamber and exhausts it out the back of the instrument. To reduce the effect of the instrument on the sample, the minimum throat diameter is 3.8 cm. As seen from this schematic, the sample chamber is in the cavity of the hybrid laser in the region between the Brewster window and the plane mirror. Light scattered from the particles in the sample area is collected by the optics shown, passed through a narrowband interference filter and focused on the signal and masked photodiodes through a beam splitter. At the same time laser radiation passing through the 0.1%-transmitting curved mirror is focused on the reference diode. The signal from the signal diode is compared to that of the masked diode. The mask is arranged to produce a shadow on the diode equivalent to the sample area. If the particle is of a correct size and is in the correct position, the voltage from the signal diode is much larger than that from the masked diode and the signal voltage is accepted and fed to a voltage divider. The amplitude of this voltage trips a flipflop whose trigger level is set by the voltage divider. This size channel is one of 15 levels. After the particle passes through the sample area, a strobe is activated and reads out the size channel that was set. To compensate for aging in the laser output, the reference diode signal voltage is also applied to the top of the voltage divider and acts as an AGC for the system. All electronics to accomplish this are contained in the active aerosol probe head. The output of a flipflop is in digital form and when strobed out is passed on a cable feeding the data-acquisition system. The probe supplied to NRL has four size ranges, as shown in the specifications (Table C1). These are automatically switched through the use of a programmable amplifier. The use of the intracavity sample area allows the measurement of small-size particles because of the high intensity in the cavity. Also, an added feature is the insensitivity of the measurement to the index of refraction of the aerosol particle.

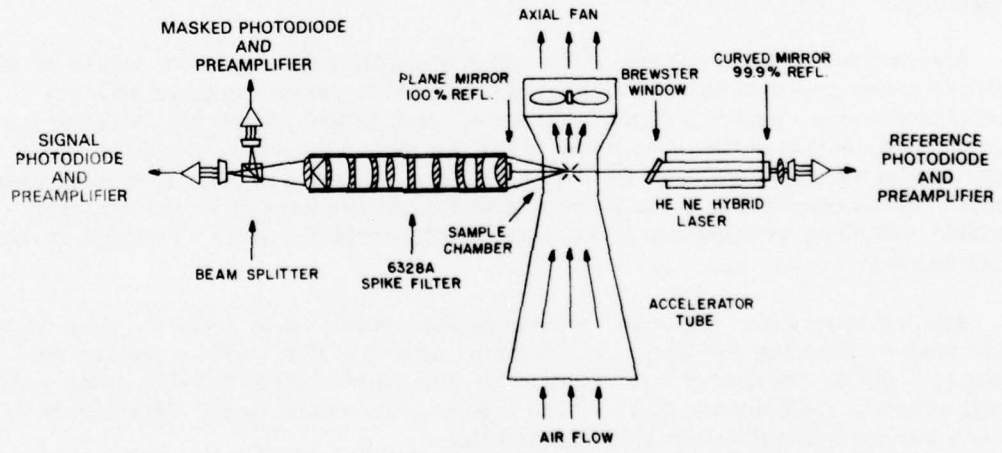

Fig. C33—Active aerosol-scattering spectrometer probe

Table C1—Specifications of the Active Aerosol-Scattering Spectrometer (Probe Subsystem)

Beamwidth	0.5 mm
Effective beamwidth	0.078 mm
Number of size channels	15
Size ranges	0.1-1.5 μm (basic range), 0.2-3.0 μm, 0.5-6.0 μm, and 0.6-8.0 μm
Minimum detectable size	0.1 μm
Size resolution	0.1 μm (basic range)
Maximum particle rate	100 kHz
Coincidence errors	Less than 10% with concentrations of 10^3 cm^{-3}
Maximum particle velocity	20 m/s
Accuracy	RMS size errors: ±10% or ± 0.1 μm, whichever is greater
Electronic detection and sizing circuitry	Two 16-channel pulse-height detectors are used to effect reject circuitry which excludes particles passing through beam edges outside the depth of field.
Depth of field	0.225 mm
Sampling Capability	Required particle sizing time is less than 10 μs. Sampling area is diamond shaped with a sampling area width of approximately 75 μm and a length of 500 μm. The sample area is a product of width and 1/2 length and is approximately 0.018 mm^2. The sample volume varies with the flow rate but is nominally 0.1 cm^3/s.

One limitation of this probe is that the larger particles tend to extinguish the laser beam, with the result that all particles beyond approximately 5 μm tend to be sized in the same channels. Because of this problem and a demonstration that a lack of larger size particles was limiting the useful information obtained in earlier measurements, it was decided to limit the probe to three ranges, dropping the largest particle range and measuring for 8 s on the next smallest range to increase the probability of obtaining counts on the larger particles. Because preliminary data show a strong effect on scattering predictions due to particles larger than 4 μm in radius, it was decided to obtain another head with a much larger sample volume to measure the larger particles. The upper limit on particle sizes of this new head will be approximately 30 μm

C6.2 Droplet Probe

There are two droplet probes which are identical except for the magnification; therefore Figs. C34 and C35 refer to both probes. Tables C2a and C2b are the specification sheets for each probe. These probes are designed primarily for use as cloud-droplet probes and are usually flown on an aircraft; hence no aspiration is provided. Because use of these probes has been limited, a performance evaluation is not available. The design of this type of probe is such that it should be unaffected by index of refraction. But one limitation to their use for ground-based fog measurements is the sensitivity of sample volume to wind motion. Fog conditions usually occur with low wind velocities; also wind currents at surface levels often are unsteady in velocity and direction, so the problem of maintaining the droplet probes in proper relation to the wind at all times and having to average measurements over long time periods to obtain reasonable counts may create an effect that will cause apparent low counts for surface operation.

Each of the two optical-array particle-size spectrometers is a custom-designed system for operations under all weather conditions. With properly installed deicing heaters the system can operate indefinitely in the varied conditions of research environments. The system is a complete spectrometer probe, its output being the particle size in binary code accompanied by a strobe pulse to increment an appropriately addressed memory channel.

Particles are sized using a linear array of photodiodes to sense the shadowing of array elements by particles passing through the field of view. Particles are illuminated by a HeNe laser and imaged as shadowgraphs onto the photodiode array. If the shadowing of each photodiode element is dark enough, a flipflop memory element is set. The particle size results from a determination of the number of elements set by a particle's passage, the size of each array element, and the magnification of the optical system.

The system as constructed contains 24 active photodiode elements and is capable of sizing into 15 size channels. (The number of active photodiode elements may vary from 17 to 24; however the maximum number of size channels resolved is 15.)

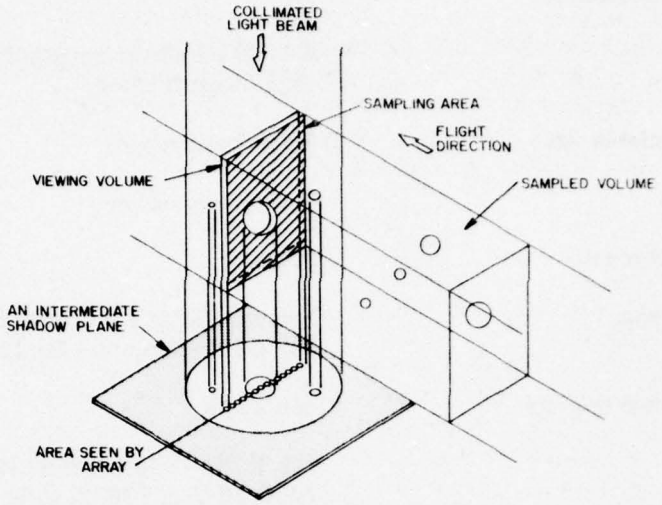

Fig. C34—Measurement volume in the optical-array spectrometer (droplet probe)

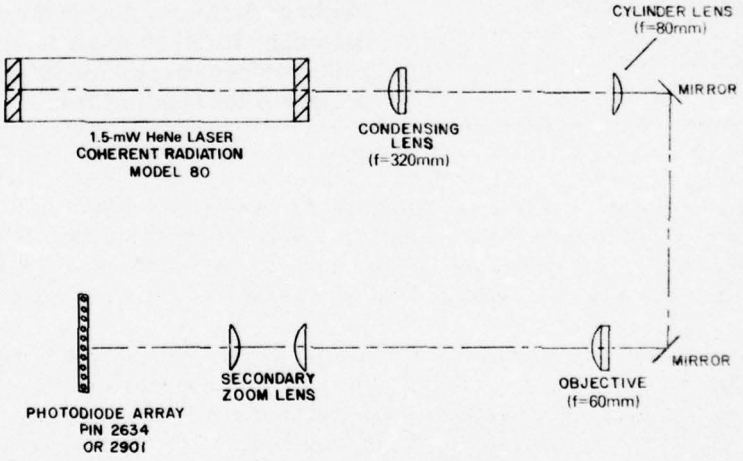

Fig. C35—Optical system for the optical-array spectrometer (droplet probe)

Table C2a—Specifications of the Optical-Array Sepctrometer (Droplet Probe) for 6-90-μm-radius Particles

Number of size channels	15
Size range	6 to 90 μm (basic range); 3 to 45 μm (high magnification)
Minimum detectable size	6 μm (basic range)
Size resolution	6 μm (basic range)
Maximum particle rate	100 kHz
Coincidence errors	Less than 0.1% with concentrations of 10^3 cm^{-3} (computed for 10-μm size)
Maximum particle velocity	250 knots
Power	115 V, 50 - 400 Hz or 60 Hz, 60 W; 70-W, 28-V or 100-W, 115-V deicing heaters
Dimensions of cylinder	71 cm long by 16.5 cm in diameter
Dimensions of optical extensions (2)	25 cm long by 2.5 cm in diameter
Weight	12.7 kg
Depth of field	Depth of field is via double threshold detection. PMS-152 photodetector module eliminates size rolloff errors at the end of the depth of field.

Table C2b—Specifications of the Optical-Array Spectrometer (Droplet Probe) for 20-300-μm-radius Particles

Number of size channels	15
Size range	2o to 300 μm
Minimum detectable size	20 μm
Size resolution	20 μm
Maximum particle rate	100 kHz
Coincidence errors	Less than 0.1% with concentrations of 10^3 cm^{-3} (computed for 10-μm size)
Maximum particle velocity	250 knots
Power	115 V, 50-400 Hz or 60 Hz, 60 W; 70-W, 28-V or 100-W, 115-V deicing heaters supplied
Dimensions of cylinder	71 cm long by 16.5 cm in diameter
Dimensions of optical extensions (2)	25 cm long in. by 2.5 cm in. diameter
Weight	12.7 kg
Depth-of-Field	*Depth of field is via double threshold* detection. PMS-152 photodetector module eliminates size rolloff errors at the end of the depth of field.

C6.3 Data-Acquisition System

The function of the buffer-memory data-acquisition system is to accumulate particle size and population information from three different Particle Measuring Systems (PMS) particle-size spectrometer probes along with other digital and analog voltage information for 1-s intervals. After each sampling period, all of the data, along with time information, are made available in the proper form (eight bits at a time) for recording on a nine-track incremental computer tape recorder. In addition, a four-digit decimal display is provided to allow monitoring of any one of the 64 words in the memory, as selected on a dual-thumbwheel word selector.

Each memory location (except parallel inputs) consists of a four-decade BCD counter (16 bits) which is simply incremented for each event that occurs during a sampling period. At the end of each sampling period, the contents of the counter are transferred in parallel into a shift register, and the counter is reset to zero for the next sample. Since transfer and reset occur in less than a few microseconds, essentially no dead time is experienced for each sample. Also, the unloading of the buffer via the shift register can be completely independent of the accumulation for each word.

Each of the three probe inputs is equipped with optical isolators on all five input signals. Four of the signals are required to code the specific size of 15 sizes from each probe, and the fifth signal provides a strobe to increment the memory location corresponding to the coded size for each particle detected by the probe. With 15 sizes for each probe, 45 memory locations are required for probe data.

Twelve analog voltage inputs are provided with each connected through a differential instrumentation amplifier to a voltage-controlled-oscillator (VCO). The output of the VCO is connected to a corresponding memory location and counts input such that the number dumped out each second will be directly proportionally to the frequency of the VCO, which in turn is directly proportional to the analog input voltage.

One memory location is used to record a 16-bit parallel input. Three memory locations are used for recording a presettable time-of-year clock and one location is used to record elapsed seconds since power on. Two memory locations are unassigned and may be used as desired in the future. The counting input to each is brought out to the parallel data input connector for external use.

The output interface provides eight data lines plus a write step and end-of-record signal for the incremental computer tape recorder. A write-error signal from the recorder is employed to provide a warning light when recording problems are encountered. Also, the ready signal from the recorder is necessary before the interface logic will enter the record mode. Actual data recording is accomplished in two bursts of about 150 ms each with 32 words per burst and two computer-tape bytes per word. This burst mode was necessary to provide adequate time for the recorder to generate an interrecord-gap (IRG) when necessary. A total of 16 data frames are recorded in each tape record, such that each record is 2048 bytes long.

A connector is provided to allow use of a standard PMS particle data system for selecting any one of the three probe inputs for independent data analysis on the CRT histogram display of size distribution.

C6.4 Particle Display Unit

The particle display unit is an active memory system designed to decode, store, and display particle-size information. This data system is of modular design and consists of a data system main frame, memory, selectable digital display, and graphical CRT size-spectra display. The selectable digital display and graphical CRT display are beneficial for real-time data monitoring requirements of precise particle counts or distribution functions.

The memory capacity is 16 addresses. Fifteen of the addresses are used for storing particle-size distribution. The remaining address can be used for other digital count information such as elapsed time or particle velocity (transit time) information. Each address has 16-bit storage capacity for 0 to 9999 counts BCD.

The data-system main frame includes all decode and addressing matrices, internal clock and data-framing electronics, digital-to-analog converter, and all selectable control functions. It provides both digital and analog high-level outputs for recording and monitoring purposes using either existing displays or peripheral recorders and printers.

C7. METEOROLOGICAL MONITORING SYSTEM

Two independent meteorological monitoring systems are in use with these experiments which consist of towers 5 m tall supporting an array of sensors whose outputs are processed and fed to two digital data-acquisition systems. Wind-speed-and-direction, refractive-index structure constant, dew-point, solar-radiometer, and barometric-pressure sensors and measurement systems are duplicated in the two meteorological systems. The van-mounted system has an atmospheric CO_2 monitor and the Particle Measuring Systems (PMS) aerosol monitoring equipment as well. The PMS data-acquisition system described in Section C6.3 is used to record aerosol counts as well as standard meteorological variables in the van-mounted system, and the fixed system uses a Monitor Laboratories Model 7200 data-acquisition system. Each system thus generates digitally recorded data tapes containing day and time identification and meteorological data. The van-mounted system data tape also includes aerosol and atmospheric CO_2 information.

C7.1 Wind Speed

Wind speed is measured by a Thornthwaite Associates Model 912 sensitive-cup-anemometer transmitter. The transmitter has been designed for sensitive operation and minimum interference to the natural flow of air past the sensor. The anemometer cups are lightweight plastic reinforced with aluminum rings, the spokes are stainless-steel tubing, and the hub is aluminum. The entire cup assemply weighs only 7 grams. The anemometer shaft is made of hardened stainless steel, and miniature ball bearings are used. A shutter mounted on the bottom of the anemometer shaft interrupts a light beam from a miniature 3-volt lamp housed in the base of the anemometer tee and focused on a photocell 12 times for every revolution of the cup assembly. A small strobe disk is provided for calibration of the wind-spread transmitters. The disk can be used to obtain a measure of the internal friction of the shaft and bearing assembly. The transmitter can be checked using the disk from time to time to determine if the transmitter requires service or cleaning. Some of the specifications for anemometer head are as follows: the

wind speed range is 0 to 1450 cm/s, the starting speed is less than 8.9 cm/s, the readout resolution (1-hour time-integrated average) is 0.1 cm/s, and the steady-state calibration equation is

$$V = 11.490 + 2.5767C - 0.000448C^2 + 0.00000028730C^3,$$

where V = cm/s and C = shaft revolutions/min. Light pulses are integrated to give a dc voltage. This voltage is displayed on a panel meter and fed to a digital data-acquisition system. The PMS system is used for the van-mounted meteorological system, and a Monitor Laboratories 7200 system is used for the fixed meteorological system.

C7.2 Wind Direction

The wind direction is measured by a wind vane that moves an arm of a potentiometer across which a regulated voltage is applied. Thus voltage is fed to a buffer amplifier and panel meter and at the same time to either data-acquisition system.

C7.3 Turbulence

The turbulence is measured by a device that used two balanced wire probes suspended in air. The probes produce an ac signal that is related to resistance changes in the wires due to temperature variations of each wire with time. This signal is amplified, and an analog of the rms logarithmic amplitude variance of the temperature difference is recorded as a voltage output using either digital data-acquisition system. Through calibration a value for the temperature-structure constant C_T is derived. This is recorded on another channel of the data-acquisition system.

This instrument is somewhat difficult to maintain in the field due to the sensitivity of the ac bridge used in the measurement, and its performance degrades when operated in an electrically noisy area.

C7.4 Dew Point

The dew point is measured by an EG&G Model 110S-M dew-point hygrometer. This is an automatically balanced model requiring little attention. The measurement range is -50°C to +50°C with an accuracy of 0.27°C. A buffered panel meter is provided to monitor the operation of the equipment. The principal of operation is to vary the temperature of a small mirror, to sense the formation of condensation on the mirror surface with an optical detector, and to measure the mirror temperature. The mirror-temperature measurement produces a voltage calibrated in degrees Celsius which is recorded by the data-acquisition system.

The Model 110S-M consists of a transmitter unit, containing the aspirated temperature and dew point sensors, a control unit, containing the sensor amplifier and signal-conditioning equipment, and 15 m of interconnecting cable (up to 120 m of cable can be used). The transmitter unit and 110-C1 control unit are designed for outdoor site installation. The 110-C3 control unit is designed for standard rack mounting on chassis slides provided with the control unit.

The dew point is measured with a primary sensor, using a Peltier-cooled mirror automatically held at the dew-point temperature by a photoresistive condensate-detecting optical system. With the mirror so controlled, the mirror temperature is determined with an imbedded platinum resistance thermometer, which then represents the true dew-point temperature. For dew points below 0°C, the system tracks the frost point. The air temperature is determined with a similar platinum resistance thermometer, mounted in a thermally shielded and aspirated thermometer well. The resistance changes of both thermometer elements are converted to millivolt or volt outputs by means of zener-diode-regulated bridge circuits located in the control unit. The installations where the data is transmitted only a short distance, the 0-to-50-mV outputs are transmitted over conventional signal circuits. For longer runs a 0-to-5-V dc signal is furnished. All output characteristics are essentially linear, and follow the Callendar-Van Dusen equation for platinum. The temperature sensors used are furnished with calibrations. As with the other meteorological variables, dew-point and air-temperature output voltages are digitized and recorded using either of the two data-acquisition systems.

C7.5 Solar Radiation

Solar radiation is measured with an Eppley Laboratory pyranometer. The instrument accepts direct radiation from the sun and diffuse radiation from the atmosphere on a series of thermocouple junctions in the form of a thermopile with the hot junctions blackened and the cold junctions whitened. These are covered with a special precision-ground hemispherical glass cover for use in all weather. The output is a dc voltage ($\approx$ 1.8 mV per J/cm^2 min) that is recorded on one of twelve analog channels of the data-acquisition system.

C7.6 Barometric Pressure

The barometric pressure is measured with a Yellow Springs Instrument Co. Model 2014-833.2/1066.91 MB-3 pressure transducer. This device employs a resistance bridge circuit which changes balance as a function of atmospheric pressure. The calibration of the device used in the mobile-van meteorological monitoring system, which spans the range 83 to 107 kPa is given by the relationships $y = 25.9667\ x + 82.049$, where y is atmospheric pressure in kilopascals and x is the ratio of the resistances measured in two arms of the internal bridge in the sensor. A dc excitation voltage is supplied to the device and produces a voltage proportional to resistance ratio and hence atmospheric pressure. This dc voltage is recorded by the PMS data-acquisition system for the van-mounted meterological system or by the Monitor Laboratories Model 7200 data-acquisition system for the fixed meteorological station.

C7.7 Atmospheric CO_2

The instrument used for monitoring the atmospheric CO_2 is a Beckman Model 215B differential absorption analyzer. The detector, which is the heart of the system, consists of a cell filled with the gas that is to be analyzed. The cell is divided into two parts by

a thin metallized diaphragm (Fig. C36) located in the left half of the cell as shown in Fig. C36 is a fixed metal button forming a capacitor with the metallized diaphragm. The two halves each have an infrared transmitting window to admit energy.

Another part of the instrument consists of two cells; one is for the sample to be measured, and the other is a reference cell to be filled with a nonabsorbing gas. The system is operated by passing infrared energy through both cells and into the detector. The cell with the nonabsorbing reference gas passes more energy into one half of the detector, expanding the gas more than the other side causing the diaphragm to flex thereby, changing the capacitance.

The variable capacitor is part of a tank circuit coupled to a 10-MHz crystal-controlled oscillator. To produce a signal, the two sources at the input of the sample and reference cells are interrupted by a 10-Hz chopper. The resultant imbalance of the detector changes the capacitance at the 10-Hz rate, detuning the tank circuit and producing an amplitude modulation of the 10-Mhz carrier. This modulated carrier is then detected using standard RF detection techniques to produce a 10-Hz signal. The signal is amplified, phase shifted, and rectified by a synchronous detector, producing a dc voltage which is recorded by the PMS data-acquisition system. No CO_2 monitor is used with the fixed meteorological monitoring system.

This instrument has two drawbacks. One is that two separate sources are used. The power of using a differential detector is lost because of possible differences in the sources. The other is that the FM character of the unbalance signal are ignored and the detuned tank circuit is used to produce AM modulation. The result is a drift-prone instrument that could have been reasonably drift free.

C8. ON-SITE DATA PROCESSING

C8.1 Current Status

Several computer programs have been developed for the on-site Nova computer system as part of a software support contract with Science Applications Inc. (SAI). Currently meteorological data is recorded on magnetic tape by two data loggers, and it is later processed (off-line) using the Nova system. The program package has the capability to read digitized raw data from tapes, to perform all necessary data conversions, and to produce average values for all measured parameters. These averages can also be tabulated and plotted. Finally the reduced data can be copied onto an industry-compatible magnetic tape, thereby allowing the data to be transfered to other computer systems.

C8.2 Modifications in Progress

Figure C37 is a block diagram of the current system, and Fig. C38 shows the planned system configuration. Three modifications in the Nova system hardware configuration are now underway. The first one involves the use of a modem and its related

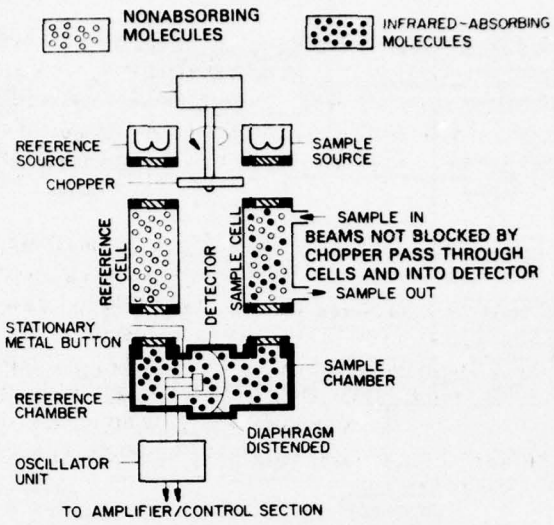

Fig. C36—Beckman Model 215 B differential absorption analyzer

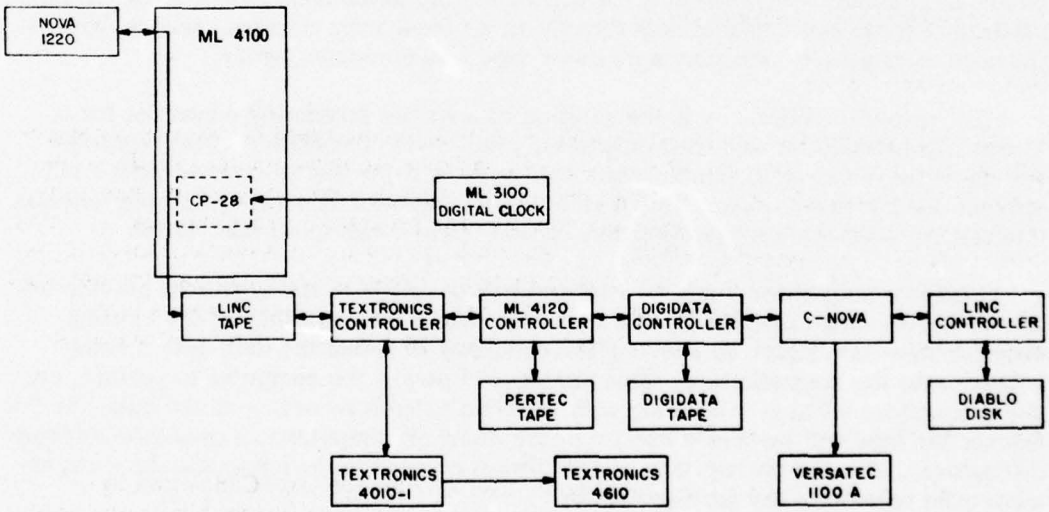

Fig. C37—Peripheral devices currently attached to the Nova on-site computer facility

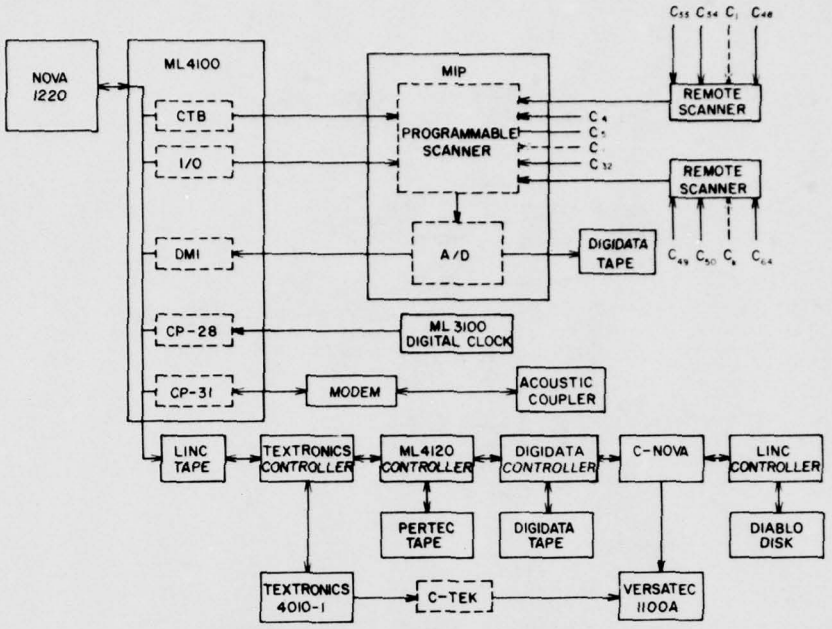

Fig. C38—Peripheral devices proposed to be attached to the Nova on-site computer facility

I/O interface which are being added to allow the Nova to communicate with other computers via standard telephone lines. It will enable the in-the-field computer to transmit partially reduced experimental data directly to a time-sharing computer service, without the need to physically transport a magnetic tape to a computer center.

The second modification is the addition of a special interfacing controller for a Versatec printer/plotter now used only in the print mode. Installation of the controller will allow the Versatee to function as a hard-copy unit for the Tektronics 4010-1 CRT terminal used with the Nova. This feature will be provided in addition to (and without interference with) the Versatec's existing capabilities as a high-speed line printer.

Finally a multichannel input peripheral will be added to the system to provide on-line data-processing capabilities. The unit will expand the capability of the existing magnetic-tape data logger by allowing the computer to access the data as it is being written onto the magnetic tape. This process will permit the computer to perform on-line calculations without interfering with the simultaneous recording of the data. In this manner the tape will serve as a backup in the event of computer failure and/or software difficulties. With the backup tape, it will always be possible to replay the day's experiment after correcting any such problems.

C8.3 Acquisition of Laser-Radiation Extinction Data

Presently, a Monitor Laboratories Model 7200 (ML 7200) data scanner is used to record 29 channels of analog meteorological data onto a digital magnetic tape for the fixed meteorological measurement system. The unit scans all of the input channels once every 3 s. The ML 7200 is now being modified to include an eight-digit BCD input from a thumbwheel switch to be located near the extinction-measurement laser control panel. The laser operator can use this switch to encode various operating parameters (such as preamplifier gain and laser line ID) for recording by the data scanner. More importantly this input will allow the operator to indicate when a laser-radiation extinction measurement is in progress. Finally the analog output from the ratiometer will be added to one of the spare input channels on the ML 7200. In this manner all of the information needed to analyze the laser data will automatically be logged onto a single magnetic tape.

For the 1976 Patuxent River NAS field operation, the on-site data reduction will be done off line. To minimize the problems associated with further software development, the existing data reduction software package (developed by SAI) will continue to be used. This package contains programs which can read the raw data tapes (containing the information recorded every 3 s) and then produce 15-min averages for an output magnetic tape. The latter tape is written in a character format that is compatible with most large-scale computer systems, and it provides a reliable method for transferring data from the minicomputer (where the data are reduced) to the time-share computer (where the data are analyzed).

One disadvantage of the earlier method was that the meteorological data averages were produced for times when no laser-radiation extinction measurements were being made. The ML 7200 modifications will allow the program which processes the raw data tapes to identify those times during which laser measurements were in progress. The program can then calculate meteorological data averages for only those time intervals needed. These meteorological averages can then be passed to the output tape along with the measured extinction signals and the other operating parameters.

Besides eliminating the problems associated with recording the meteorological data separately from the laser-radiation extinction data, the new procedure will also reduce the quantity of data that needs to be transferred to the time-share computer. For handling this smaller quantity of data, a modem can be used to transmit the data directly to the time-share computer via standard telephone lines. Thus the intermediate output tape can be eliminated, and the overall performance of the system will be further enhanced.

Finally a computer output option is available for the ML 7200 which can expand the unit's capabilities to allow a computer to access the input data channels as they are being scanned and recorded on the magnetic tape. This procedure provides a method for developing on-line data-reduction capabilities while simultaneously maintaining the ability to record the original data on tape. By performing the on-line data acquisition through the data scanner, a backup tape (containing all the raw data) will always be available in the event of computer failure. Since the data logger is a key part of future plans for on-line data processing, adding the laser operating parameters to the ML 7200 will benefit not only current plans for off-line processing but will simplify the changeover to on-line processing as well.

C9. TELEMETRY SYSTEM

Because of the large distances between the two ends of the path and because field operations are often conducted in semiremote areas, the process of combining the data obtained at each end of the path has always presented special problems. The GaAs optical data link was installed in 1975 to ease some of these problems. While it did simplify the procedure needed to obtain optical extinction measurements, neither its speed nor its bandwidth are suitable for the quantity of data which must be transmitted from one end of the path to the other.

To improve the overall flexibility of the field measurement program, a high-speed telemetry system was acquired. Figure C39 is a block diagram of system components. The telemetry system contains a scanner and an A/D converter which encodes input analog signals at one end of the path (using an NRZ-S code format) and then transmits them via a microwave link to the opposite end. At the receiver end of the path, these digital signals are reconverted to produce analog output voltages. The microwave system has sufficient bandwidth to support both the telemetry system and a video channel.)

The telemetry link, which is now undergoing final testing, will be phased into the field operations gradually. When used in conjunction with the data input channel of the minicomputer, this combination will allow the system to monitor data channels at both ends of the experimental path. In addition to data transmission the telemetry system will also include some channels specifically dedicated for instrument control purposes. Thus it is expected that the computer will not only be able to monitor equipment at the opposite end of the path, but will eventually be used to control such devices as well.

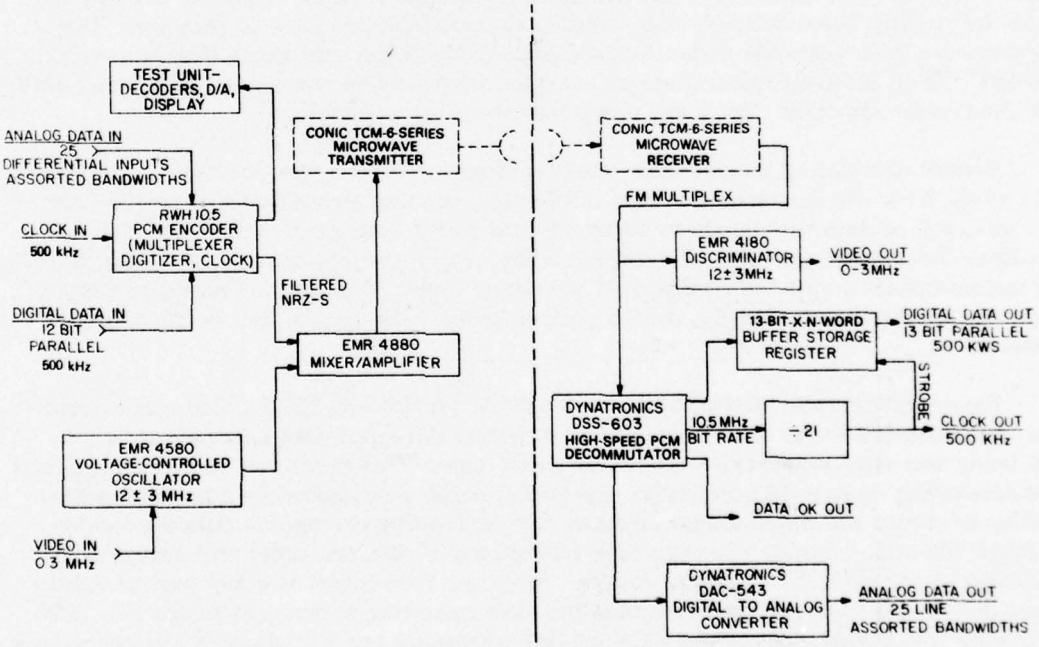

Fig. C39—High-speed telemetry system

Appendix D

PROJECT STAFFING

The atmospheric-transmission measurement program at NRL is conducted by the Optical Radiation Branch and is currently staffed by members of both the Experimental Propagation and the Laser Aerosol Interaction Sections of the Branch. Peter B. Ulrich, NRL Code 5560, served as acting Branch Head during the major portion of the time that this document was prepared. An organizational chart showing those portions of the Optical Radiation Branch directly concerned with this project is shown in Figure D1.

Joseph A Curcio, Branch Senior Scientist, is involved in all areas of the project, providing the benefit of experience gained during many years of conducting a wide variety of optical measurements in the atmosphere. James A. Dowling, Head of the Experimental Propagation Section, is Project Officer for the project and has served in that capacity during the previous field programs in Florida and California. Gary T. Trusty, Head of the Laser Aerosol Interaction Section, has been actively engaged in the measurement and predictive modeling of optical effects due to atmospheric aerosols in connection with the Florida and California experiments. Not shown in Fig. D1 are contractor personnel who perform certain vital functions associated primarily with mechanical, electronic, and meteorological monitoring tasks supporting the project.

Personnel resumes for the individuals shown in Fig. D1 follow.

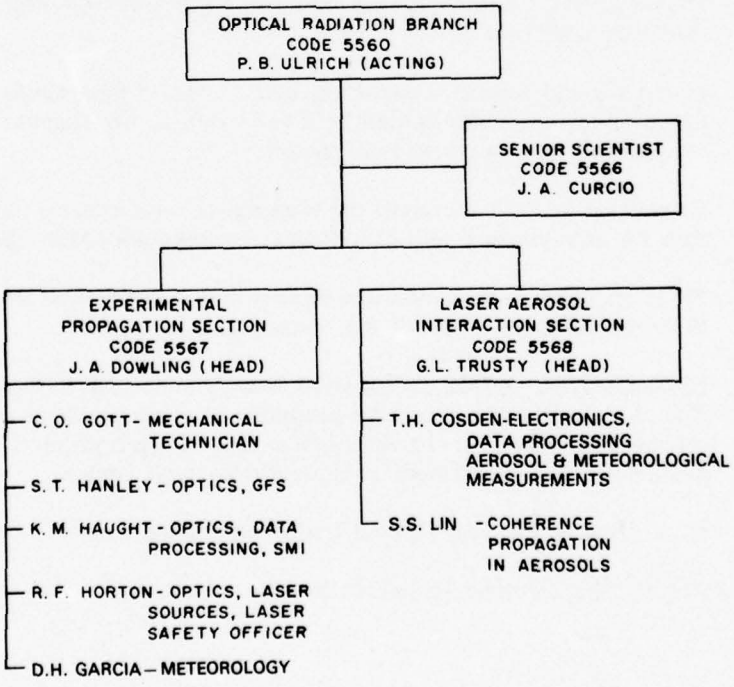

Fig. D1—Staffing organization for the atmospheric measurement program

RESUME FOR PETER B. ULRICH

Physicist, GS-14.
Acting Branch Head, Optical Radiation Branch, Code 5560;
Propagation Theory Section Head, Code 5565, Optical Radiation Branch.

Education

B.S., Physics — 1959 — Yale University.
Ph.D., Physics — 1966 — Massachusetts Institute of Technology
Thesis: "The Non-Landau Singularities of Feynman Graphs."

Experience

1959 - 1962 Officer, USN, Assigned to NRL Electron Beams Branch, Nucleonics Division. Theoretical work on intense electron beams and relativistic Brillouin flow.

1962 - 1967 Physicist, NRL, part-time, ibid. Studied linear and two-sheet beams, and feedback transducers.

1962 - 1966 Instructor and Research Assistant, MIT. Studied large-single-crystal growing methods and color centers in alkali halides. Investigated beam-plasma interactions and quantum field theory.

1965 - 1967 Consulting on helical coaxial cable design (Phelps Dodge) and data reduction for astrophysical and geophysical experiments (Amer. Sci. and Engr.).

1967 - 1970 Physicist, NRL. Conducted theoretical and experimental work on the Sozotron intense-electron-beam storage ring.

1970 - 1974 Physicist, NRL Optical Propagation Branch (since 1973, Optical Radiation Branch). Developed computer programs to solve problems of propagating intense laser beams in the atmosphere and directed projects on multiple-pulse code, two-wavelength code, and defocused beams.

1974 - 1976 Head, Theory Section, Optical Radiation Branch.

1976 - present Acting Head, Optical Radiation Branch.

Publications and Professional Activities

Nine articles in reviewed journals on relativistic electron beams and laser beam propagation in the atmosphere.
Six NRL Reports on laser beam propagation.
Four NRL Radiation Project Progress Report articles.
Six NRL Radiation Quarterly Nuclear Science and Technology articles.
One NRL Report of Progress article on Relativistic Brillouin Flow.
Three NRL Memorandum Reports on relativistic electron beams.
Thirty-one articles for NRL HELP Quarterly Reports.
Twenty-one technical addresses presented at various symposia and program reviews.
Two NRL publication awards.
Chairman, NRL Committee to Select Time-Sharing Computer.
Member, NRL Research Computation Committee, 1970-1971.
Member, Optical Society of America.
Member, Sigma Xi.
Listed in American Men of Science since 1966.

RESUME FOR JOSEPH A. CURCIO

Physicist, GS-14
Senior Scientist, Code 5566, Optical Radiation Branch.

Education

B.S., Chemical Engineering — 1942 — Villanova College (physics, chemistry, math — chief credits); Laser Propagation through the Atmosphere — 1967 — Ohio State University.

Experience

1942 - 1945 Chemist, Industrial Test Laboratory, Frankfort Arsenal.
1946 - 1968 Physicist, NRL Optics Division.
1969 - present Physicist, NRL Optical Sciences Division, Optical Propagation Branch (since 1973, Optical Radiation Branch); Head, IMORL Field Operations Section. Conducts theoretical and experimental research on the optical properties of the lower atmosphere, including scattering, absorption, and signal transmission.

Publications and Professional Activities

Over 100 articles, papers, reports, and oral presentations on original research concerning atmospheric transmission, scintillation, scattering, and absorption of IR to UV wavelengths including incoherent and laser sources.

Ten articles in NRL HELP Quarterly Reports.

Nationally recognized authority on atmospheric optics and laser propagation.
Past Chairman of the Atmospheric Technical Council of the Optical Society of America.
Fellow, Optical Society of America (OSA).
President, National Capitol Section, OSA, 1974.

RESUME FOR JAMES A. DOWLING

Physicst, GS-13
Linear Propagation Section Head, Code 5567, Optical Radiation Branch.

Education

B.S., Physics — 1961 — Catholic University of America.
Ph.D., Physics — 1967 — Catholic University of America
Thesis: "A Study of Line Shapes for CO Infrared Emission Lines."
Minors: E. E. and math.
Graduate courses in Scientific Russian and quantum electronics.

Experience

1967 - 1968 Avco, staff scientist. Optical communications; rapid scan spectrometry.

1968 - 1973 Physicist, Optical Propagation Branch. Studies of the optical properties of the atmosphere, including turbulence, absorption, scattering, and extinction; applications of interferometric techniques; laser-beam-quality diagnostics.

1973 - Present, Head, Linear Propagation Experiments Section; Optical Radiation Branch Project Officer, NRL Low Power Laser Propagation Studies, Cape Canaveral Fla. and TRW Capistrono Test Site.

Publications and Professional Activities

Five jouranl publications on IR emission lines, laser pumping light sources, and focused beams in atmospheric turbulence.
Three NRL reports on atmospheric transmission experiments.
Twelve articles in NRL HELP Quarterly Reports.
Fourteen presentations on atmospheric propagation of optical/laser beams.
Member NRL Laser Safety Committee, 1974.
Member, Optical Society of America (OSA).
Member, OSA Tellers Committee, 1972.
OSA judge at local science fairs, 1970, 1972.

RESUME FOR CHARLES O. GOTT

Engineering Technician, GS-8.
Linear Propagation Section, Code 5567, Optical Radiation Branch.

Education

Calvert County High School
1961 - 1967 State of Maryland, maintenance all types of vehicles.
1967 - 1974 NRL. maintenance of vehicles, Transportation Section, CBD.
1974 - present NRL, Optical Sciences Division. Install and maintain vaccuum and gas systems for lasers. Plan and design Mechanical parts for optical trailers. Plan and control field installations for propagation measurements.

Publications

Three NRL reports on atmospheric transmission experiments.

RESUME FOR STEPHEN T. HANLEY

Physicist, GS-12.
Linear Propagation Section, Code 5567, Optical Radiation Branch.

Education

B.S., Physics — 1967 — University of Washington.
M.S., Physics — 1970 — University of Washington.
Ph.D., Physics — 1973 — University of Washington.
NRL Selected Student for Special Graduate Study Program.
Thesis: "Absolute Calibration of an Optical Detector by Cascade Coincidence Counting and Measurement of NO_2 Continuum Rate Constant Near 6402Å."

Experience

1968 - 1970 NRL Physicist summer employee, Applied Physics Branch. Space-object photoimaging; high-photon-flux interaction with hydrogen; laser-induced heat transfer computer program solution, including phase transition in one- and two-dimensional models using finite-difference approach.

1973 - present NRL Optical Engineering Branch (since 1973, Optical Radiation Branch), Optical Sciences Division. Measurement analysis and improvement of NTSL beam quality; field measurements of DF laser line optical extinction; NTSL gas analysis computation and optimization.

Publications and Awards

Memorandum for File: "Application of Photographic Imaging to Space Object Identification,"
One NRL report: "A General Solution to the One- and Two-Dimensional Melting Using a Finite Difference Approach."
Review of Scientific Instruments 43, 1339 (1972): "Angular Correction to Absolute Photometric Calibration by Photon Coincidence,"
One article for NRL HELP Quarterly Report: "Gas Mixtures and Handling for Gas Dynamic Lasers."
NRL Memorandum Report: "Beam Quality Measurements on the NTSL."
Three NRL reports on atmospheric transmission experiments.
Phi Beta Kappa.
Graduate Cum Laude.
Member, American Physical Society.
Member, Optical Society of America.

RESUME FOR KENNETH M. HAUGHT

Physicist, GS-12.
Linear Propagation Section, Code 5567, Optical Radiation Branch.

Education

B.S., Physics — 1970 — The University of Akron.
M.S., Physics — 1971 — The Ohio State University
Masters Problem: "An Interferometer Control System Using a Laser Standard."
Ph.D., Physics — 1975 — The Ohio State University
Dissertation: "A Vacuum Infrared Spectrograph with a Digital Data System and an Improved Technique for Wavenumber Assignment."

Experience

1973 - 1975 Laboratory of Molecular Spectroscopy, The Ohio State University. Construction of a 6-meter vacuum spectrograph. High-resolution molecular absorption studies of key atmospheric constituents.

1975 - 1976 Electro-Optics Division, Science Applications Inc, Data reduction and analysis for NRL laser atmospheric transmission measurements.

1976 - present Optical Radiation Branch, NRL Optical Sciences Division. Fourier transform Spectroscopy. Software systems development and numerical analysis. Atmospheric propagation field experiments. EO instrumentation design.

RESUME FOR RICHARD F. HORTON

Physicist, GS-12.
Linear Propagation Section, Code 5567, Optical Radiation Branch.

Education

B.S., Physics — 1968 — Case Western Reserve University.
M.S., Physics — 1973 — American University.
Graduate studies, physics — 1968 to present — American University. Completed most courses and examinations for doctorate.
Thesis: "Rayleigh Scattering from Relaxation Processes in Fluids from 1-7000 Atmospheres" (work done at NRL, Code 8130).

Experience

1968 - 1973 Naval Weapons Laboratory. Detection and imaging of CO_2 laser radiation using cholesteric liquid crystals, 1968-1970. Reflection distribution function measurements using CO_2 laser, 1971-1972.

1973 - present NRL Optical Radiation Branch, Optical Sciences Division. Preparation and calibration of a DF chemical laser, and conducting of propagation field experiments.

Publications

Three NRL reports on atmospheric transmission experiments
One journal article, "Depolarized Doublet Spectra of Toluene at High Pressure."
Two NWL reports on laser imaging using liquid crystals and on laser reflectance measurements.
One patent, No. 3,723,739 on imaging of laser radiation using liquid crystals.

RESUME FOR DANIEL H. GARCIA

Electronics Engineer, GS-11,
Linear Propagation Experiments Section, Code 5567, Optical Radiation Branch.

Education

B.S., Electrical Engineering — 1966 — University of Florida.
M.A., Physics — 1970 — University of South Florida
Thesis: "An Experimental Study of the Luxembourg Effect in Low-Density Plasmas."

Experience

1966	General Electric Company, Apollo Support Department. Operations research; automated documentation system; human performance assessment; biomechanics systems.
1966	Sperry Microwave Electronics Company. Avionics automated checkout equipment and testing procedures.
1968 - 1969	Instructor, The Citadel military college. Instructor in undergraduate physics courses.
1970 - 1975	Electronics Engineer, Technical Information Division, Naval Research Laboratory. Technical editor of scientific/engineering formal reports.
1976	Electronics Engineer, Optical Sciences Division, Naval Research Laboratory. Development and operation of meteorological systems; development of data-reduction techniques and software for analysis of meteorological data.

Publications

"Measurements of Body Motions," Am. Soc. Mech. Engineers publication #66/WA/BHF-2.
"Biomechanics Data for Man Amplifiers," *Mechanical Engineering*, August 1967.
"Nonresonant Nonlinear Wave Interaction in Slightly Ionized Ar and AR-Hg Plasmas," Bull. Am. Phys. Soc., Vol. 15, Ser. 2, 1309 (1970).
Two NRL reports on atmospheric transmission experiments.

RESUME FOR GARY L. TRUSTY

Physicist, GS-12.
Laser Aerosol Interaction Section Head, Code 5568, Optical Radiation Branch.

Education

B.S., Electrical Engineering — 1964 — University of Cincinnati
M.Sc., Electrical Engineering — 1966 — Ohio State University
Thesis: "Scintillation in 3.5-Micron Laser Propagation."
Ph.D. Electrical Engineering — 1972 — Ohio State University

Dissertation: "Absorption Measurements of the 10.4-Micron Region Using a CO_2 Laser and a Spectrophone."

Experience

1964 - 1965 Systems Research Labs., Dayton, Ohio. Research on saturable dye Q switches with ruby lasers and 3.5-μm laser propagation.

1966 - 1973 Electroscience Laboratory, Ohio State University. Construction of CO_2 and Nd:YAG lasers and operation of chemical lasers. Investigation of 1.06-μm laser propagation in the atmosphere. Theoretical calculations of lifetimes of some levels of several atoms and of CO laser lines through the atmosphere.

1974 - present Planning and executing experiments involving propagation of various laser wavelengths through the atmosphere, analyzing the resulting data, and preparing scientific reports.

Honors and Publications

Eta Kappa Nu.
Sigma Xi.
Eight papers on lifetimes of various atomic states and on atmospheric propagation and absorption of certain lines of CO_2 and CO lasers, as articles in IEEE, JOSA, technical reports for OSU, USAF, and presentations at OSA meetings.
Three NRL reports on atmospheric transmission experiments.

RESUME FOR THOMAS H. COSDEN

Electronic Development Technician, GS-12.
Laser Aerosol Interaction Section, Code 5568, Optical Radiation Branch.

Education

Annapolis High School, 1943.
Radio Engineering and Maintenance School, U.S. Coast Guard, 1945.

Experience

1946 - 1948 NRL, Radio Division II, Radar Tracking Section. Install, operate and maintain radars.

1948 - 1950 NRL, Radio Division I, Radar Propagation Section. Radar Target Area Measurements

1950 - present NRL Optics Division. Optical Propagation and radiation measurements in the visibile and infrared regions. Under water optical propagation measurements.

Publications

Twenty-three NRL reports on optical sea Hering, underwater optical propagation and atmospheric transmission experiments.

RESUME FOR SAMUEL S. C. LIN

Research Physicist, GS-13.
Laser Aerosol Interaction Section, Code 5568, Optical Radiation Branch.

Education

B.S., Mechanical Engineering — 1961 — National Taiwan University, Taiwan, China.
M.S., Aeronautical Sciences — 1964 — University of California, Berkeley.
Ph.D., Engineering Physics — 1972 — University of California, San Diego
Thesis: "An Experimental Study of Gasdynamical Turbulence "
Fields of Study: physics, fluid mechanics, physical gasdynamics, plasma physics, quantum electronics, optics, and applied math.
Postdoctoral Research — 1972-1974 — Optical radiation propagation in turbulent media; image degradation through turbulent media.

Experience

1961 - 1962 Ensign, Chinese Navy.

1964 Technical Staff, National Engineering and Sciences Co., Water Waves.

1964 - 1966 Preliminary Design Engineer, AiResearch Manufacturing Co. Designs in turbines, compressors, heat exchangers, supersonic combustion ram-jet engines, turbofan jet engines, and thrust nozzles.

1966 - 1972 Research Assistant, University of California, San Diego. Design and development of a variable-density subsonic wind tunnel for gasdynamic turbulence studies, instrumentation and data-reduction systems.

1972 - 1974 Assistant Research Engineer, University of California, San Diego. Image degradation by turbulent media; information retrieval from speckle images.

1974 - 1976 Staff Member, M.I.T., Lincoln Laboratory. High-power laser effects, hot-spot tracking and signature studies, active laser radar imaging and tracking, and laser radar power amplifier (LRPA).

1976 - present Research Physicist, Optical Radiation Branch, NRL. light-scattering studies, coherence propagations, optical communications, and fiber ring interferometer.

Publications and Professional Society

Two journal publications on gasdynamic turbulence.
Two meeting reports on gasdynamic turbulence.
One journal article on image degradation by turbulent medium.
One meeting report on imaging degradation.
Member, Optical Society of America.

Appendix E

PROJECT PREPARATION AND PERFORMANCE SCHEDULE

Tasks, procurement actions, and other items identified with the preparation and execution of this project are listed along with other pertinent information in Table E1. The task numerology listed in Table E1 has been divided into three levels for convenient organization. Task identification numbers are given in the first column, along with a description of the task. The designation of the individual or group primarily responsible for the task and the estimated cost are given in the second and third columns respectively. The period of performance planned for task conpletion as of approximately 15 March 1976 is indicated by open triangles and continuous horizontal lines with an update current to the completion of the draft of this report, namely through 1 September 1976. It is anticipated that further updates of this schedule will be included in supplements to this report to be generated as this program continues.

Table E1—Task Performance Schedule for Preparation and Execution of the NRL Atmospheric Propagation Measurements Program, Initiated March 1976
(Updated to Sept. 1976: △——△ indicates the original dates;
---△ indicates a shift to an updated estimated date;
▲ indicates a completed milestone)

Task No. and Item	Responsible Individual or Activity	Est. Cost (10^3)	Schedule (1976) Mar 29	Apr 5	Apr 12	Apr 19	Apr 26	May 3	May 10	May 17	May 24	May 31	June 7	June 14	June 21	June 28	July 5	July 12	July 19	July 26	Aug 2	Aug 9	Aug 16	Aug 23	Aug 30	Sept 6
1. Transmitter																										
1.1 GFCS source																										
1.11 Delivery	SH	86K																								
1.12 Installation	RH shop	200																								
1.2 JA monochrometer																										
1.21 *Mounting*	RH shop	200																								
1.22 Calibration	RH WA	NC																								
1.3 Fluorine system																										
1.31 *Overhaul regulator*	CG outside	250																								
1.32 Order spare	CG JC	NC																								
1.33 Rework charcoal reactor	WA shop	375																								
1.34 Install rollers in F_2 enclosure	WA shop	375																								
1.35 Check out F_2 safety system	CG	NC																								
1.4 Vacuum system																										
1.41 Order oil and spare parts	CG JC	750																								
1.42 Order soda lime	JC	250																								
1.43 Repair soda-lime trap	WA shop	100																								
1.44 Assemble, check out vacuum system	CG WA	JC																								
1.5 Gas supplies																										
1.51 Reorder needed gases	CG JC	1000																								
1.52 Modify gas-system housing	CG shop	125																								
1.6 Optics																										
1.61 Check and recoat as needed	KH JC	300																								
1.62 Protection for optical surfaces	JC	500																								
1.63 Cleaning facility for XMTR mirror	CG shop	200																								
1.7 CO/CO_2 laser																										
1.71 Install molectron laser	CG	NC																								
1.72 OSU CO laser																										
1.721 *Procurement*	JD	NC																								
1.722 Construction	Ron Long	36K																								

Table continues

Table E1—Task Performance Schedule for Preparation and Execution of the NRL Atmospheric Propagation Measurements Program, Initiated March 1976 (Updated to Sept. 1976: △——△ indicates the original dates; ---△ indicates a shift to an updated estimated date; ▲ indicates a completed milestone) (Continued)

Task No. and Item	Responsible Individual or Activity	Est. Cost (10^3)	Schedule (1976)
			Mar 29 | Apr: 5, 12, 19, 26 | May: 3, 10, 17, 24, 31 | June: 7, 14, 21, 28 | July: 5, 12, 19, 26 | Aug: 2, 9, 16, 23, 30 | Sept: 6
1. Transmitter (continued)			
1.73 Check liquid N_2 storage bottles	CG	NC	
1.74 Check/repair liquid N_2 valves	CG	100	
1.75 Rework exhaust of CO_2 vacuum system	CG/WA	200	
1.76 Order spares for coolant pumps	CG/JC	100	local supplier
1.8 Miscellaneous			
1.81 Check out power meters	WA	NC	
1.82 Install microwave electronics	WA shop	100	
1.83 Check and replace tires	CG/JC	500	GSA delivery
1.84 Order vacuum cleaner	JC	100	e.g., Hoover
1.85 Provide storage area for air packs	CG shop	125	
1.86 Order, install gas-cylinder winch	JC/CG shop	500	delivery; installation; canceled
1.87 Beef up power outlets and mount	WA/JC	200	
1.88 Rearrange front-end storage	CG shop	600	
1.89 Construct wall rack	CG shop	100	
1.90 Mount warning light	WA	50	
1.91 Install remote control for radio	WA	150	
1.92 Make adaptor for elevation screw	CG shop	300	
1.93 Install jacking tabs for optical bench	CG shop	300	
1.94 Clean up stands for transmitter	CG shop	225	
1.95 Order dehumidifier and spare	CG/JC	300	delivery
1.96 Check out data link	JC	NC	
1.97 Prepare checklist for transmitter operation	RH	NC	
2. Receiver			
2.1 Optics			
2.11 Design specifications	RH/KH	NC	
2.12 Place orders			
2.121 Ellipse	RH	2200	SORL
2.122 Small parabola	RH	500	Mufolletto Optical Co.
2.123 Flats (4)	RH	200	Mufolletto Optical Co.
2.124 Spherical mirrors (GFS)	RH	50	Mufolletto Optical Co.
2.125 Newtonian diagonals (4)	RH	200	Mufolletto Optical Co.
2.13 Check and resurface optics as needed	KH/JC	200	outside optical shop
2.14 Protection for surfaces	JC	500	Mufolletto Optical Co.
2.2 Mounts			
2.22 Construction	RH/shop	200	
2.24 Spider construction	RH/shop	800	
2.3 Alignment aids			
2.31 HeNe laser installation	RH	NC	
2.32 Aperture installations	RH shop	500	
2.4 Scanning Michelson Interferometer			
2.41 On-the-job training	KH	NC	at Carson
2.42 Delivery	KH	114K	Carson Systems, Newport Beach; delivery of SMI head; delivery of all hardware
2.43 Installation	KH shop	300	rescheduled
2.44 Initial testing	KH	NC	graybody source
2.45 Integrate with optics	KH/RH	NC	
2.5 Gas filter spectrometer			
2.51 Delivery	SH	86K	
2.52 Installation	SH shop	300	rescheduled
2.53 Initial testing	SH	NC	rescheduled
2.6 Extinction detectors			
2.61 Testing and optimization	JC/RH/WA	NC	
2.62 Place orders—Pyroelectrics	JC	600	Laser Precision, Inc.
2.7 Miscellaneous			
2.71 Modifications	KH	(Design)	
2.711 Porch cover	CG/shop	2500	
2.712 Table underpinning	CG/shop	1500	
2.713 Extension	CG/shop	2500	
2.72 Order vacuum cleaner	JC	200	e.g., Hoover
2.73 Construct ladder	WA shop	500	
2.74 Install remote control for radios	WA	75	
2.75 Install radio antenna	WA	NC	

Table continues

Table E1—Task Performance Schedule for Preparation and Execution of the NRL Atmospheric Propagation Measurements Program, Initiated March 1976 (Updated to Sept. 1976: △——△ indicates the original dates; ---△ indicates a shift to an updated estimated date; ▲ indicates a completed milestone) (Concluded)

Task No. and Item	Responsible Individual or Activity	Est. Cost (10^3)	Schedule (1976)
			Mar 29 | Apr: 5, 12, 19, 26 | May: 3, 10, 17, 24, 31 | June: 7, 14, 21, 28 | July: 5, 12, 19, 26 | Aug: 2, 9, 16, 23, 30 | Sept: 6
2. Receiver (continued)			
2.76 Clean up stands	CG/shop	225	△—▲ delivery
2.77 Order dehumidifier	JC	150	△——▲ delivery
2.78 Check out data link	JC	NC	△——▲
2.79 Order cart for toilet waste	CG/JC	100	△——△ canceled
2.80 Comfort facilities	CG/shop	300	△——△----------▲
3. Meteorological			
3.1 Receiver			
3.11 Relocate in office trailer	WA	NC	△—▲
3.2 Dew-point			
3.21 Installation of panel mtr	JD/FRI	NC	△——▲
3.22 Add new DP; fix hardware/software	GT/KH	NC	△——▲
4. Electronics			
4.1 Extinction measurement			
4.11 Order PAR ratiometer	JD	1800	△——▲
4.12 Order PAR lock-in amp	KH	8000	△——▲
4.13 Complete RWH electronics documentation	JD/PRI		△——▲
5. Data Processing			
5.1 Extinction experiment			
5.11 Automate data acq.	KH	NC	△—▲
6. Site Preparation			
6.1 CBD			
6.11 Modify sites	CG/PW	700	△—▲
6.12 Increase electrical pwr.	CG/PW	800	△——▲
6.2 Local overwater site			
6.21 Selection	Group	NC	
6.22 Approvals	JD/DF	NC	△——△----------▲
6.23 Road modifications			
6.231 Road modifications RCVR site	JD/DF	500	△——△ canceled
6.232 Road modifications XMTR site	JD/DF	700	△——△ canceled
6.24 Electric power			
6.241 Checkout both sites	JD/DF	NC	△—△
7. Miscellaneous			
7.1 Check air cond., office trlr	CG/shop	400	△——▲
7.2 Repair pump, trlr door	CG/shop	125	△—▲
7.3 Check portable-radio batt.	CG	200	△—▲
7.4 Repair elec. trailer roof	CG/shop	125	△——▲

*U.S. GOVERNMENT PRINTING OFFICE:1977 240-824/255 1-3